

1. INTRODUCTION AND EXPLANATORY NOTES, LEG 89¹

M. Baltuck, Geology Department, Tulane University
R. Moberly, Hawaii Institute of Geophysics, University of Hawaii
and

S. O. Schlanger, Department of Geological Sciences, Northwestern University²

INTRODUCTION

Because drilling during the DSDP-IPOD program had not yet succeeded in sampling Jurassic sediments from the Mesozoic superocean, remnants of which remain in the western Pacific, Leg 89 was designed to recover sediments of probably Bathonian–Callovian age (150–160 m.y. old). Recovery of such sediments would enable us to compare Mesozoic superocean strata and paleoenvironmental conditions with Atlantic sediments, paleoenvironments of similar age, and coeval strata deposited along Tethyan continental margins—now exposed in Tertiary fold belts.

Primary Scientific Objectives

Major paleoceanographic changes occurred when the configuration of the continents and oceans evolved from a pattern dominated by a single supercontinent and a single superocean to one of fragmented continents and several oceans. These oceanographic changes included the transition from a warm to a cold ocean, the occurrence of periods of pronounced oxygen deficiency (oceanic anoxic events) in deep or mid-water ocean environments with related changes in ocean chemistry, and the evolution of major marine plankton groups that probably altered the pathways of major elements such as calcium, silicon, carbon, and phosphorus. The creation, consumption, and possible temporary isolation of marginal seas and ocean basins appear to have led to chemical fractionation and sudden environmental changes. The history of these events prior to 100 Ma is still poorly known.

The modern western Pacific Ocean represents a remnant of the early Mesozoic superocean, whereas the Atlantic and Indian Oceans are relatively newly developed. The oldest sediments reached to date by drilling are late Callovian and were cored at Site 534 (Blake-Bahama Basin) on Leg 76. Results from this site indicate that early Callovian sediments were deposited in a restricted basin. In the later Callovian and Oxfordian, the first opening of a worldwide ocean pathway linking the Tethys and Pacific oceans occurred. In the Pacific, the oldest sedi-

ment drilled in the ocean floor is latest Jurassic or earliest Cretaceous. Therefore we lack knowledge of earlier Jurassic Pacific sediments that could substantiate this opening or record its effects.

The Middle Jurassic pelagic sediment record derives primarily from sections outcropping in the Tertiary fold belts, which correspond to Tethyan continental margins in various stages of evolution; sediments that contain this record have never been sampled from any deep oceanic basin. A major controversy centers on whether or not these sections can be regarded as truly representative of the early Mesozoic world ocean. A consequence of this enormous gap in our knowledge is that all biostratigraphic data from the early Mesozoic remain biased toward fossil assemblages from nearshore and marginal areas of ocean basins in the early stages of their evolution.

There is ample evidence from magnetic data (Fig. 1) that portions of the oceanic crust in the western Pacific are at least as old as Middle to possibly Early Jurassic, but no complete record of the sediment sequence overlying the oceanic crust in this area has been obtained so far. Deep Sea Drilling Project and geophysical data also suggest that these portions of the seafloor were actually generated at moderate to low latitudes in the Southern Hemisphere away from any large continental landmass. We expected that this Mesozoic sediment record could be recovered at Site MZP-6 (Leg 89, Site 585) in the deep East Mariana Basin (Fig. 2A illustrates a predicted lithologic column based on seismic reflection profiling).

The specific paleoenvironmental questions to be addressed on Leg 89 include the following:

1. How did the early evolution and radiation of the oceanic plankton (coccoliths, radiolarians, benthic and planktonic foraminifers) influence the composition of pelagic sediments, and how do these fauna and flora reflect Mesozoic ocean chemistry?

2. Did the opening of the North Atlantic Ocean affect the circulation and chemistry of the world ocean in a manner similar to that which has been proposed for the opening of the South Atlantic?

3. Are "pelagic" sediments exposed in Tertiary fold belts (ribbon radiolarites, ammonitico rosso, etc.) characteristic of open ocean environments?

4. Can we establish an early Mesozoic pelagic bio- and magneto-chronology?

5. Were the mid-Cretaceous sedimentary environments in the deep Pacific better oxygenated than those in the Atlantic and Indian oceans?

¹ Moberly, R., Schlanger, S. O., et al., *Init. Repts. DSDP, 89*: Washington (U.S. Govt. Printing Office).

² Addresses: (Baltuck) Geology Department, Tulane University, New Orleans, LA 70118; (Moberly) Hawaii Institute of Geophysics, University of Hawaii, 2525 Correa Rd., Honolulu, HI 96822; (Schlanger) Department of Geological Sciences, Northwestern University, Evanston, IL 60201.

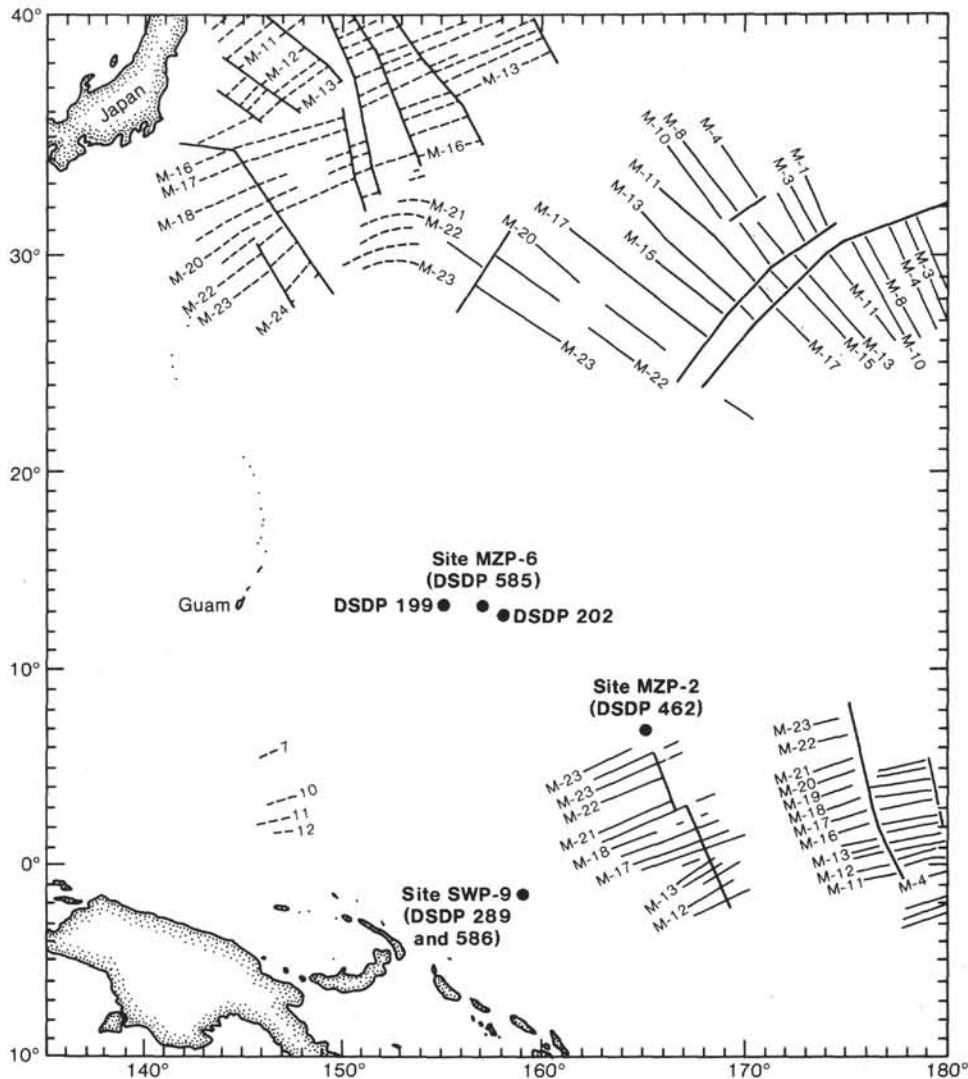


Figure 1. Map of Leg 89 sites showing magnetic lineations in the western Pacific.

Although numerous outstanding Mesozoic paleoenvironmental objectives such as the nature of the Cretaceous/Tertiary boundary, the mechanisms behind mid-Cretaceous oceanic anoxic events, the occurrence of water exchange with partially or completely isolated basins, the structure and stability of deep water masses, and the chemical fractionation between major ocean basins remain important problems in other oceanic basins, the basic objective of Leg 89 was the recovery of a truly oceanic sediment record, which is only preserved in the western Pacific.

Secondary Scientific Objectives

One of the major results of DSDP and IPOD drilling has been the discovery in the central and western Pacific basin of large amounts of volcanic rock that were emplaced on the lithospheric plate in an off-ridge, intra-plate setting. Off-ridge volcanism, referred to as mid-plate volcanism here, resulted in formation not only of linear island chains but also clusters of seamounts and deep-water sill-flow complexes. Dating of this midplate volcanism by isotopic and biostratigraphic methods in-

dicates that in the western Pacific widespread volcanism took place between about 110–115 and 70 Ma. Until quite recently the vertical component of plate motion was considered largely in terms of lithospheric cooling, thickening, and subsidence as a function of the age of the oceanic lithosphere. It has now been suggested by a number of workers that the subsidence path of a large portion of the Pacific oceanic lithosphere has diverged significantly over long periods of time from an ideal Parsons-Sclater curve because of reheating of the lithosphere subsequent to its formation at a ridge crest. We need to quantify the vertical component of plate motion resulting from this reheating effect and to determine the temporal and spatial extent of thermally induced bathymetric highs.

In order to address the problem of midplate volcanism, we proposed a contingency to early completion of MZP-6 and the deepening of Site MZP-2 (DSDP Site 462, Nauru Basin). Drilling at Site 462 on Leg 61 revealed the presence of a Cretaceous sill-flow complex at least 500 m thick (Fig. 3). Analysis of scenarios for the possible vertical-motion history of the Nauru Basin suggested that

the bottom of the sill-flow complex could be as little as 50 m below the total depth (1068.5 m) reached at Site 462 on Leg 61. Time permitting, we proposed that Site 462 be reentered and deepened, with the objectives of penetrating the complex and thereby obtaining the data with which to identify the vertical-motion history of the site and also to sample the underlying Mesozoic sediments.

A further objective of Leg 89 was to reoccupy DSDP Site 289 as IPOD Site SWP-9 (Leg 89, Site 586). This was planned, upon the request of the JOIDES Planning Committee, in order to minimize the steaming time on Leg 90. We drilled several holes using the hydraulic piston corer (HPC) at Site 586 in order to recover a complete Neogene section. Physical property data from the Site 289 cores indicated that a penetration of 250 m could be expected. After the necessary shipboard measurements were made, the cores taken were saved for the Leg 90 scientific party for workup as part of their leg report. Cores from Holes 586, 586A, and 586C are described by Leg 89 scientists. Cores from Hole 586B were split and described by Leg 90 scientists. The graphic descriptions of cores from all holes at Site 586 are included in the Site 586 report, this volume.

PRINCIPAL RESULTS

Site 585

Drilling Holes 585 and 585A resulted in a maximum penetration of 763.7 m in Hole 585; a misfit core barrel sub resulted in loss of the hole. Hole 585A was terminated at 892.8 m because of complete bit failure. Fifty-five cores were taken from Hole 585 and 22 from 585A. Figure 2B illustrates a reinterpretation of seismics based on results of coring (Fig. 3).

The sedimentary section that was recovered is dominated by redeposited volcanogenic material in middle Cretaceous strata and redeposited fossils in Upper Cretaceous and Neogene strata. Compared to most open ocean sites, the rocks are relatively unfossiliferous and the faunal and floral diversity is low. The intensive reworking and general paucity of the autochthonous fossils made the task of assigning a precise zone to each core difficult. Many biostratigraphic zones were recognized; it appears that the section is largely complete from middle Eocene to upper Aptian with minor hiatuses, although evidence for the presence of most of the Paleocene is lacking and upper and middle Maestrichtian assemblages occur only redeposited within Tertiary strata.

Although the Jurassic objectives were not reached, information derived from Holes 585 and 585A revealed the following:

1. Benthic foraminiferal faunas indicate that the East Mariana Basin was at abyssal depths from the Aptian to the present.
2. Intense edifice-building volcanism took place in the area during the Aptian through the middle Albian. The timing of the onset of volcanism is not known.
3. Volcanic edifices around the basin reached to or above sea level and were capped or fringed by carbonate reefs and banks in the Aptian-Albian.

4. The growth of these edifices provided the bathymetric relief needed for the delivery to the abyssal Mariana Basin of the numerous and thick turbidite sequences that dominate the sedimentary section.

5. Organic carbon-rich sediments formed in the basin at or very close to the Cenomanian/Turonian boundary; these carbonaceous sediments are the local record of a global oceanic anoxic event.

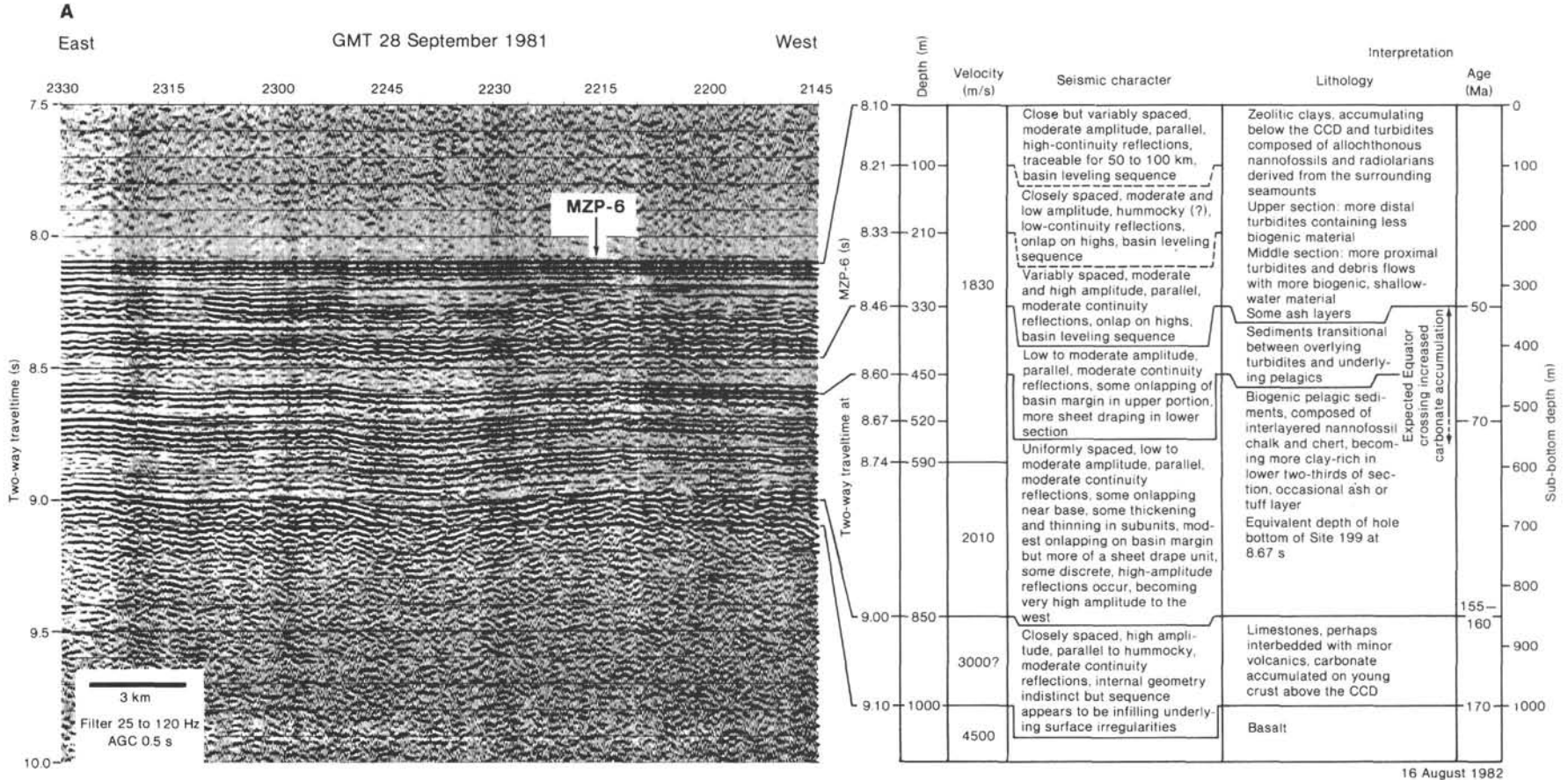
6. The Pacific Plate moved from a paleolatitude of 15.0°S in the late Aptian-Albian, through 7.0°S in the Turonian-Santonian and 1.0°S in the Maestrichtian-Paleocene before reaching its present latitude of 13.5°N at Site 585.

7. The prominent reflector previously interpreted as basement at 9 s in the East Mariana Basin is midplate Aptian volcanoclastic strata. This state of affairs may hold true for much of the western Pacific.

Site 462

Our initial operation after a successful reentry with a logging and clean-out bit was to log while lowering a temperature-logging tool as deeply into the old hole as possible. It met with very slight obstructions at 470 and 515 m depth, and was blocked at 521 m. The tool was retrieved, and the drill string used to clean out the hole down into the basalt sills below 560 m. No difficulty was encountered, and so the drill string was tripped from the hole. A regular BHA (bottom hole assembly) and bit were run down on the drill string. The hole was reentered, and pipe was then run to the bottom of the hole, flushing out carefully en route, until the bit reached bottom. The total depth at the end of Leg 61 was 1068.5 m; the drillers now reported a depth of 1071.7 m. The 3.2-m discrepancy may have resulted from a mismeasurement of pipe during either Leg 61 or this leg or both. Possibly some or all of the discrepancy resulted from a temporary change of sea level related to the 1982 El Niño event, and recorded at several tide gauges in the western Pacific (personal communication, Klaus Wyrki, 1985). So as not to have to change all the records of Leg 61 cores, yet to be able to use the length of the present drill string from drill floor to bit for present measurements, we decided that the first core (Core 93) would be cut less than the usual 9 m, and any discrepancy included within the amount of recovered versus not-recovered rock.

Eight cores were cut with the bit (Fig. 4). The volcanic sequence cored in this 140.5-m interval is composed of an alternating series of aphyric and moderately aphyric flow basalts containing various proportions of clinopyroxene, plagioclase, and olivine as phenocryst phases. The basalt flows represent the continuation downward of the lower flows (type B basalts) found during Leg 61, the lowest of which was designated as Unit 44, and are divided into 11 volcanic units, 45 through 56. The thicker volcanic units commonly are aphyric holocrystalline or glassy basalts and in some cases represent a packet of rapidly extruded smaller cooling units. The thinner volcanic units are often quench-textured throughout and represent individual flows. Except for a questionable occurrence of pillow structures in Unit 51 (Core 462A-104), all of the units are apparently sheet flows.



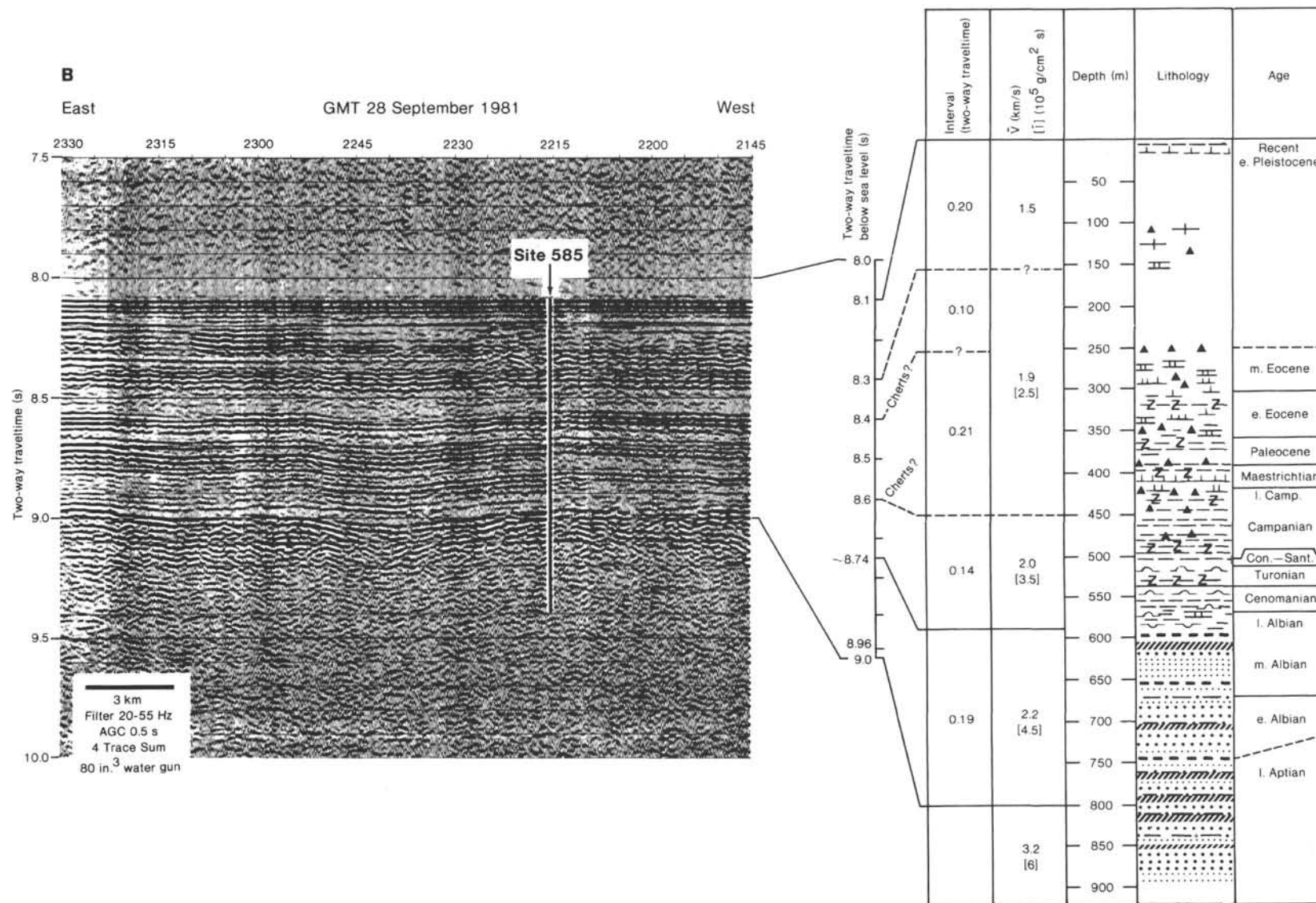


Figure 2. A. Predicted lithologic column at Site MZP-6 based on multichannel seismic line (Shipley et al., 1983). B. Revised geologic column incorporating drilling results.

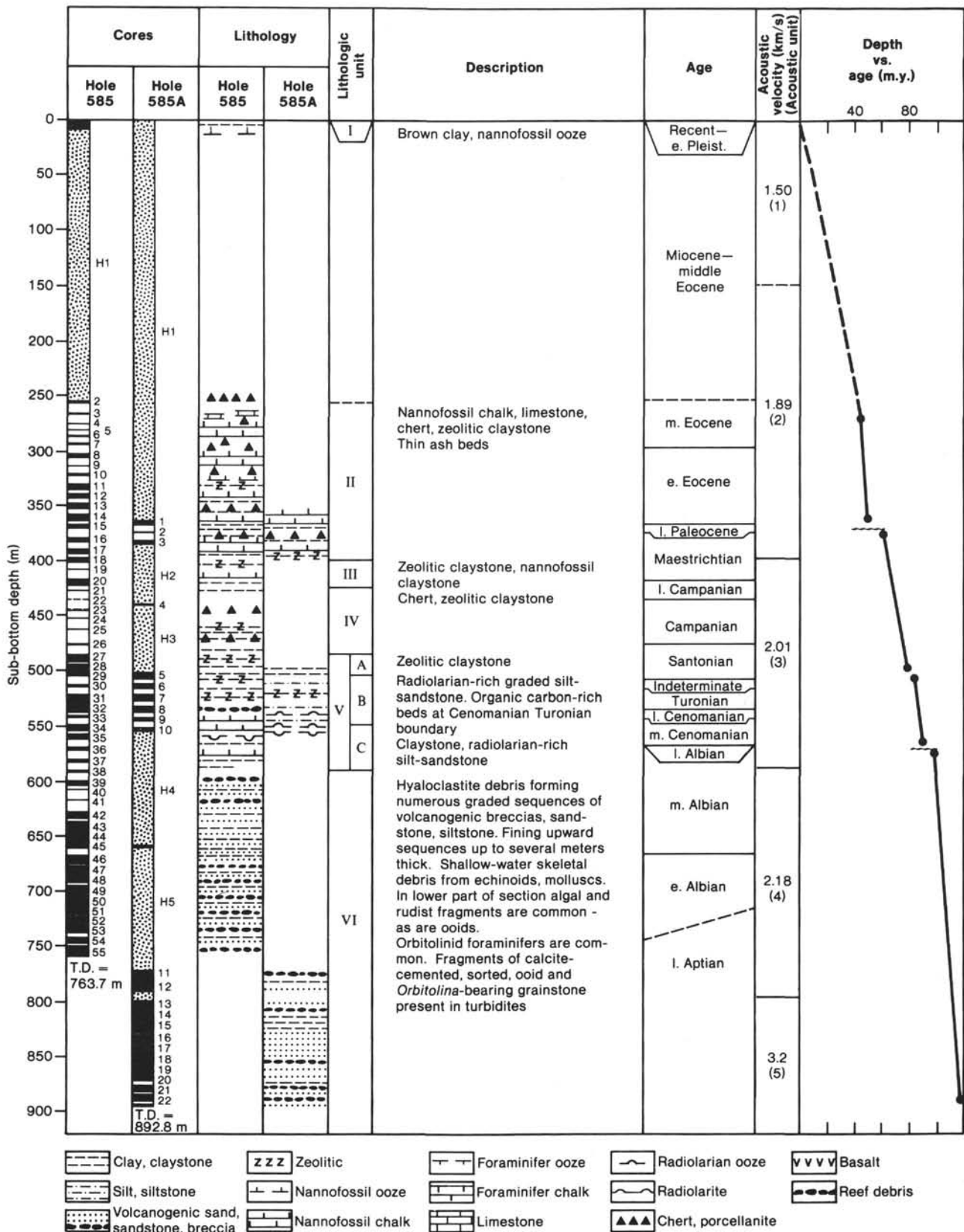
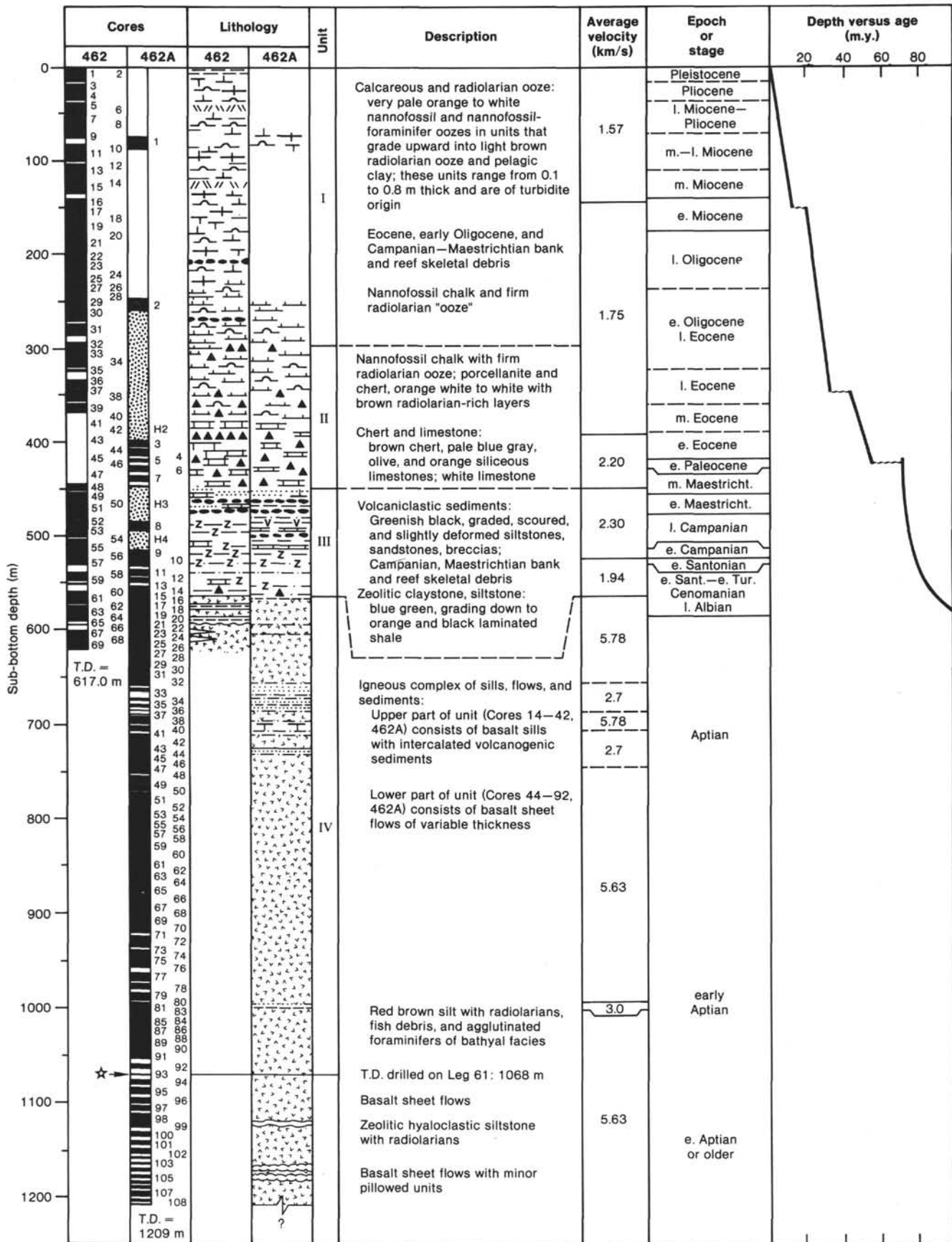


Figure 3. Columnar section at Site 585 showing: cored intervals (black), intervals without core recovery (white), and washed intervals (stippled); lithologic units; ages; seismic interval velocities; and depth versus age.



Although glass and olivine are characteristically replaced by brownish smectites through the basaltic pile, the degree of alteration is generally low. No fresh glass remains, although palagonite is present in a few cases. Alteration took place in the lower zeolite facies under slightly acid to mildly alkaline, low CO_2 -activity, reducing conditions.

In Section 462A-100-1 a few centimeters of zeolitic hyaloclastitic sediment were recovered in contact with a chilled, glassy margin of a basalt flow. Radiolarians from this sediment include *Holocryptocapsa hindei*, which has a range from uppermost Jurassic to lowermost Aptian.

Shipboard revision of radiolarian-based age determinations of Cores 462A-46 and -80 is significant. Core 462A-46 was thought to be Aptian-Barremian. It is now thought that the sediment is Aptian in age but contains a reworked Berriasian fauna. Core 462-80 was thought to be Barremian but now is interpreted to be of the late early Aptian; the sediment also contains a reworked Early Cretaceous (pre-early Hauterivian) radiolarian fauna. These revisions are important because they show that older sediments are in the vicinity.

Paleomagnetic data were obtained from 35 minicores that were analyzed using progressive alternating field (AF) demagnetization. A steep positive inclination (probably an artifact of the drilling and exposure to the steel drill pipe) was overprinted on a primary negative inclination in every sample. Because the site was south of the equator during the Cretaceous, this implies that the entire basalt flow complex is of normal polarity. The inclinations are tightly grouped within individual flow units, and these cluster means range from $-51.2^\circ (\pm 1.5^\circ)$ to $-10.7^\circ (+1.5^\circ)$.

The mean inclination of the magnetic units could be distinctly identified as $-35.9^\circ (\pm 7^\circ)$, implying a paleolatitude of $19.9^\circ\text{S} (\pm 5^\circ)$. This is comparable to the paleolatitude of the overlying basaltic complex drilled on Leg 61 of $20.6^\circ (\pm 2.4^\circ)$ (recalculated from Steiner, 1981). The two nearly identical mean paleolatitudes imply that northward movement of the site was insignificant during the emplacement of the igneous complex. Resetting of the thermal remanent magnetism at the tops of some units to match that of the overlying unit is good evidence, along with the chilled margins, that these layers are flows, not sills.

A temperature log was run in Hole 462A for several reasons: (1) the hole had remained undisturbed for 4.25 yr. since Leg 61 and presumably was at thermal equilibrium; (2) there was some uncertainty in the interpretation of the logs run in 1978; and (3) there remains the question whether heat flow values become constant with age or decrease as a function of the square root of age. The results of the temperature log run on Leg 89 showed that seawater is flowing down into the hole at a rate of about 1700 l/hr. This downhole flow condition is similar to that described at DSDP holes in young crust. At Site 462 the downward flow is interpreted as a forced convection due to pore-fluid underpressure in the sediment column above the basalt sill-flow complex and not the result of hydrothermally driven circulation. This raises

the interesting question as to the origin of underpressure in the deep-sea sediment sections.

Although Jurassic sediments were not reached at this site, the hole remains clean, the reentry cone is easily seen on the reentry scanning tool, and the sediment layers in the sill-flow complex show that there are older sediments than Aptian in the Nauru Basin; conditions are propitious for a return to the site when a longer drill string can be deployed.

Site 586

We approached old Site 289 from the northeast and dropped an acoustic beacon at the dead-reckoning position of the site at 0527 hr. on 19 November. The PDR (precision depth recorder), mud-line cores in two holes, and the gamma-ray log runs gave different depths to the seafloor. We decided to use as datums for all holes the gamma-ray measurement of 2218 m from the drill floor (2208 m from sea level), which was close to the 2207 PDR determination corrected to sea level, and the filled second mud-line core, which indicated the seafloor to be above 2219.4 from drill floor, but which is shallower than the 2223.1 mud line determined in the first hole.

The first hole was cored with the HPC to 44.4 m and had to be abandoned there when the inner core barrel holding what would have been Core 6 broke off while extended below the bit. We then started Hole 586A by washing to 44.4 m and then continuously coring. We reached 305.3 m total depth, with 98.5% recovery. The 586 and 586A cores were split, described, and sampled. A second set of continuous HPC cores was taken to 240.3 m in Hole 586B, with 97.8% recovery. This set was stored unsplit, along with the earlier split cores, for the use of Leg 90. The descriptions given by the Leg 90 scientific party of the cores from Hole 586B are included in the Leg 90 volume.

Hole 586C was rotary drilled to 623.1 m, with one spot core at its total depth, to provide a borehole for logging. An excellent suite of Schlumberger sonic velocity, spontaneous potential, induction, density, gamma ray, and caliper logs was obtained.

The 503-m section recovered is Quaternary to upper Miocene and consists of foraminifer-nannofossil ooze that became chalky below about 260 m. The fossil contact and the type of preservation of the foraminifers suggest that these sediments are not the result of a purely pelagic "rain." Allochthonous shallow-water faunal elements and mixtures of abraded specimens with specimens having delicate structures preserved occur throughout the cored section. Figure 5 gives a summary lithologic column of Site 586.

Most of the studies of the HPC cores from Site 586 will be by Leg 90 personnel and will appear in the Leg 90 volume.

EXPLANATORY NOTES

Authorship

Authorship of the site reports is shared collectively by the Shipboard Scientific Party, with ultimate responsi-

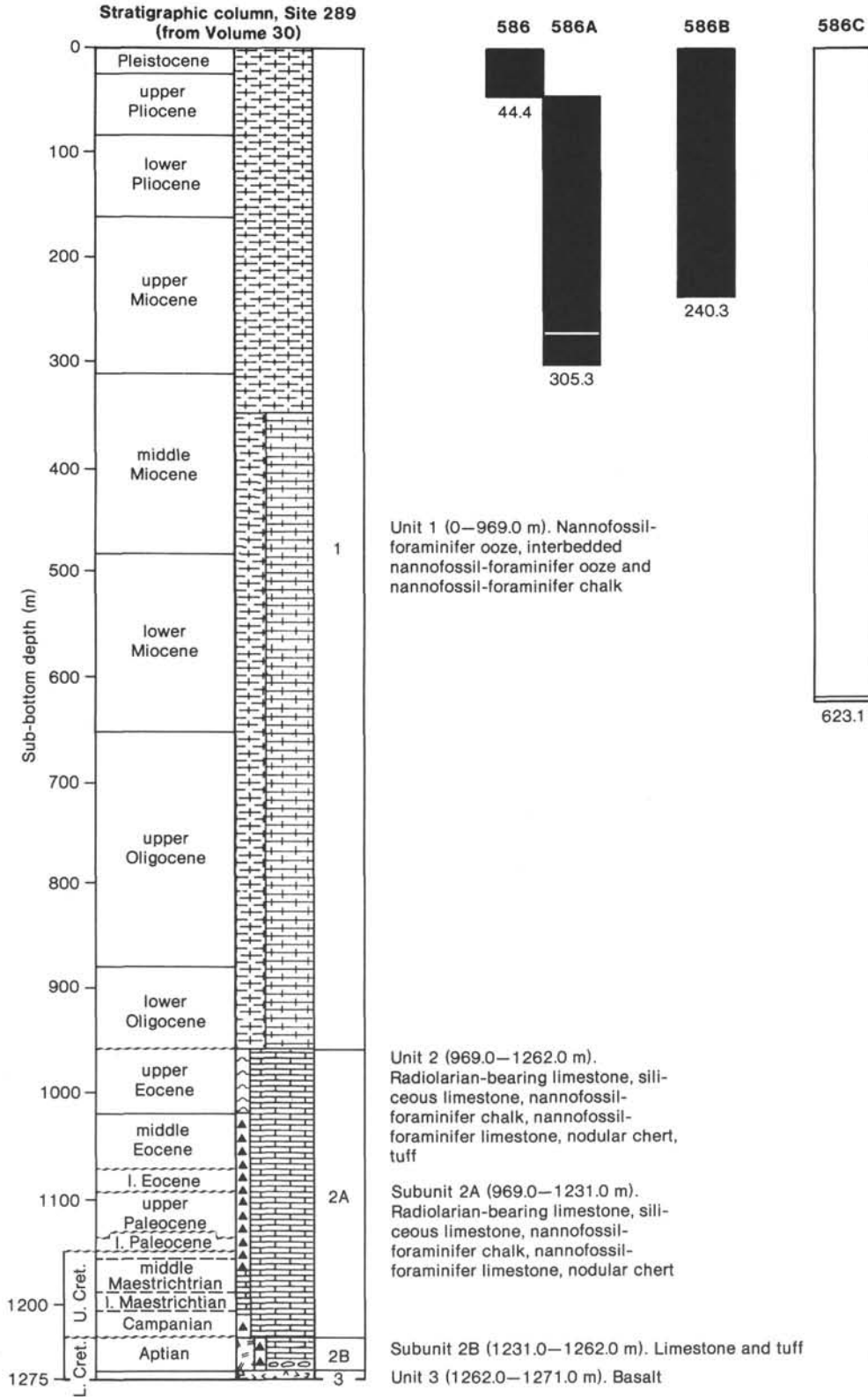


Figure 5. Columnar section at Site 586.

bilities lying with the two Co-Chief Scientists. The site reports follow the same general outline (authors responsible for each section are indicated in parentheses):

Site Summary Data and Principal Results	(Moberly and Schlanger)
Background and Objectives	(Schlanger and Moberly)
Operations	(Moberly and Schlanger)
Lithology	(Baltuck, Dean, Haggerty, Whitman, Floyd—Site 585; and Moberly—Hole 462A; and Ogg—Site 586)
Biostratigraphy	(Bergen, Premoli Silva, Schaaf, and Sliter)
Sedimentation Rates	(Bergen, Premoli Silva, Schaaf, and Sliter)
Organic Geochemistry	(Schaefer)
Inorganic Geochemistry	(Julson)
Igneous Petrology	(Floyd)
Paleomagnetism	(Ogg)
Physical Properties	(Fujii)
Logging and Downhole Measurements	(Fujii, Schlanger, and Moberly)
Seismic Stratigraphy	(Schlanger and Moberly; and Whitman [Site 585])
Summary and Conclusions	(Moberly and Schlanger)

Survey and Drilling Data

The survey data used for specific site selections are given in each site report. On passage between sites the standard Deep Sea Drilling Project geophysical surveying gear was used. This consisted of a magnetometer, 12-kHz echo sounder for bathymetry, 3.5-kHz reflection profiles for discriminating shallow sub-bottom sediment reflectors, and an air-gun system for deeper penetration reflection profiling: two simultaneously triggered air guns of 60- and 120-in.³ capacity. Reflections are received from the streamed hydrophone array transmitted to two recorders operating at different scales and the same filter setting. A newly operational water gun of Scripps design was used in surveying the last site (586). Continuously recorded depths were read on the basis of an assumed 1463 m/s sounding velocity. The sea depth (in meters) at each site was corrected (1) according to the tables of Matthews (1939), and (2) for the depth of the hull transducer (6 m) below sea level. In addition, any depths referred to the drilling platform have been calculated on the assumption that this level is 10 m above the water line.

Drilling Characteristics

Because water circulation down the hole is open, cuttings are lost onto the seabed and cannot be examined. The only available information about sedimentary stratification between cores, other than from seismic data, is

from an examination of the behavior of the drill string as observed on the drill platform. The harder the layer being drilled, the slower and more difficult it is to penetrate. There are, however, a number of other variable factors that determine the rate of penetration, so it is not possible to relate this directly to the hardness of the layers. The parameters of bit weight and revolutions per minute are recorded on the drilling recorder and influence the rate of penetration.

Drilling Deformation

When the cores were split, many showed signs of the sediment having been disturbed since its deposition. Such signs were the concave-downward appearance of originally plane bands, the haphazard mixing of lumps of different lithologies, and the near-fluid state of some sediments recovered from tens or hundreds of meters below the seabed. It seems reasonable to suppose that this deformation came about during or after the cutting of the core. Three different stages during which the core may suffer stresses sufficient to alter its physical characteristics are: cutting, retrieval (with accompanying changes in pressure and temperature), and core handling.

Shipboard Scientific Procedures

Numbering of Sites, Holes, Cores, and Samples

DSDP drill sites are numbered consecutively from the first site drilled by *Glomar Challenger* in 1968. A site number, slightly different from a hole number, refers to one or more holes drilled while the ship was positioned over one acoustic beacon. These holes could be within a radius as great as 900 m from the beacon. Several holes may be drilled at a single site by pulling the drill pipe above the seafloor (out of one hole), moving the ship 100 m or more from the previous hole, and then drilling another hole. The first (or only) hole drilled at a site takes the site number. A letter suffix distinguishes each additional hole at the same site. For example: the first hole takes only the site number; the second takes the site number with suffix A; the third takes the site number with suffix B, and so forth. It is important, for sampling purposes, to distinguish the holes drilled at a site, because recovered sediments or rocks from different holes usually do not come from equivalent positions in the recovered stratigraphic column.

The cored interval is measured in meters below the seafloor. The depth interval of an individual core is the depth below seafloor at which the coring operation began to the depth at which the coring operation ended. Each rotary coring interval is generally 9.1 to 9.2 m long, which is the nominal length of a core barrel, but the coring interval may be shorter. "Cored intervals" are not necessarily adjacent to each other, but may be separated by "drilled intervals." In soft sediment, the drill string can be "washed ahead" with the core barrel in place, but not recovering sediment, by pumping water down the pipe at high pressure to wash the sediment out of the way of the bit and up the space between the drill pipe and wall of the hole. However, if thin, hard rock layers

are present, it is possible to get "spotty" sampling of these resistant layers within the washed interval, and thus have a cored interval greater than 9.2 m.

Cores taken from a hole are numbered serially from the top of the hole downward. Core numbers and their associated cored interval in meters below the seafloor are normally unique for a hole. Material from a washed interval (as just described) is distinguished from normal coring recovery by the prefix "H" and a number to designate the washed interval; for example, "H3" at Hole 585A could contain material from the washed interval of 447.7 to 502.6 m sub-bottom; it occurs between rotary Cores 4 and 5.

Full recovery for a single rotary core is normally 8.8 m of sediment or rock, which is in a plastic liner (6.6 cm I.D.), plus about a 0.2-m-long sample (without a plastic liner) in the core catcher. The core catcher is a device at the bottom of the core barrel that prevents the core from sliding out when the barrel is being retrieved from the hole. The sediment core, which is in the plastic liner, is then cut into 1.5-m-long sections and numbered serially from the top of the sediment core (Fig. 6). When full recovery is obtained, the sections are numbered from 1 through 7 (the last section is shorter than 1.5 m). The core-catcher sample is placed below the last section when the core is described, and labeled Core Catcher (CC); it is treated as a separate section (for sediments only).

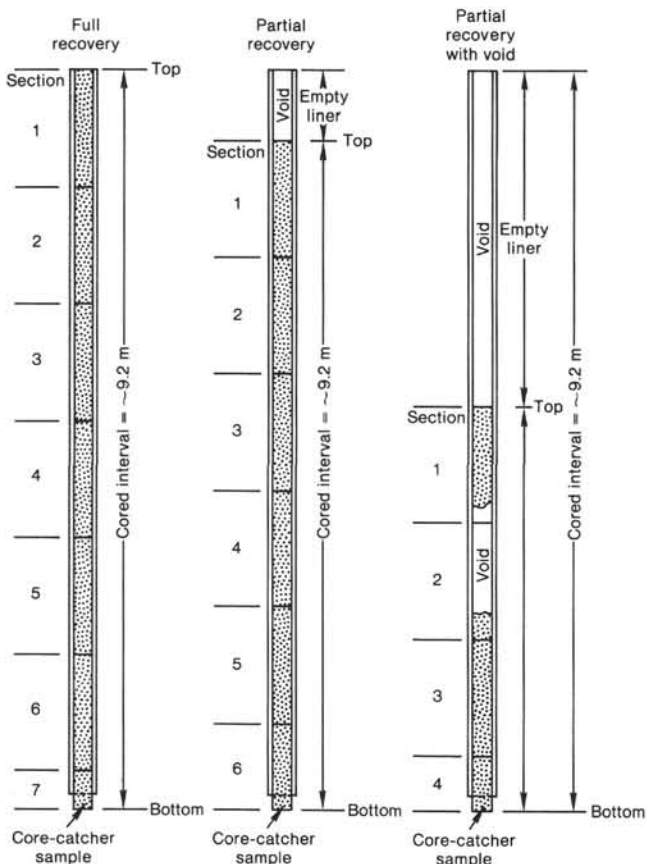


Figure 6. Diagram showing procedure in cutting and labeling of core sections.

When recovery is less than 100%, and if the sediment is placed in the top of the cored interval, then 1.5-m-long sections are numbered serially, starting with Section 1 at the top. There will be as many sections as needed to accommodate the length of the core recovered (Fig. 6); for example, 3 m of core sample in plastic liners will be divided into two 1.5-m-long sections. Sections are cut starting at the top of the recovered sediment, and the last section may be shorter than the normal 1.5-m length.

When recovery is less than 100%, the original stratigraphic position of the sediment in the cored interval is unknown; we conventionally attribute the top of the recovered sediment to the top of the cored interval. This is done for convenience in data handling, and for consistency. If the core is fragmented with less than 100% recovery, and if shipboard scientists believe that the fragments were not originally contiguous, then sections are numbered serially and the intervening sections are noted as void, whether the fragments as found were contiguous or not.

A sample is designated by the distance in centimeters it spans as measured from the top of the section from which it is taken. A full identification number for a sample consists of the following information: leg-site, (or hole)-core-section, interval in centimeters from the top of the section. For example, the sample identification number "89-585A-16-3, 98-100 cm" means that a sample was taken between 98 and 100 cm from the top of Section 3 of Core 16, from the second hole drilled at Site 585 during Leg 89. A sample from the core-catcher of this core is designated "89-585A-16,CC (8-9 cm)."

The depth below the seafloor for a sample numbered "89-585A-16-3, 98-100 cm" is the sum of the depth to the top of the cored interval for Core 16 (827.0 m) and the 3 m included in Sections 1 and 2 (each 1.5 m long) and the 98 cm below the top of Section 3. The sample in question is located at 830.98 m sub-bottom, which in principle is the sample depth below the seafloor (sample requests should refer to a specific interval within a core section, rather than the depth below seafloor).

Conventions regarding the cataloguing of the hydraulic piston cores are the same as those for the rotary cores. Generally at Site 586 a full 9.5- to 9.6-m-length stroke was attempted with nearly complete recovery of core. Toward the bottom of the hole at Hole 586A frictional resistance to the removal of the core barrel from the sediment reached 30- to 50,000 lb., and to lessen the risk of structural failure the drillers changed to a 5-m stroke.

Handling of Cores

A core was normally cut into 1.5-m sections, sealed, and labeled; the sections then were brought into the core laboratory for processing. The following determinations were normally made before the sections were split: gas analysis, thermal-conductivity analysis (soft sediment only), and continuous wet-bulk density determinations using the Gamma Ray Attenuation Porosity Evaluator (GRAPE).

The cores were then split longitudinally into "working" and "archive" halves, either by wire cutter or by "super-saw." The contrast in appearance between cores

cut by the two methods can be significant. Samples extracted from the "working" half included those for measurement of sonic velocity by the Hamilton Frame method, measurement of wet-bulk density by a GRAPE technique, carbon-carbonate analysis, measurement of calcium-carbonate percentage (carbonate bomb), geochemical analysis, paleontological studies, and other studies. When sufficiently firm, the archive half was washed on the cut surface to emphasize the sedimentary features. The color, texture, structure, and composition of the various lithologically different parts of a section were described on standard visual-core-description sheets (one per section), and any unusual features were noted. Two or more smear slides were often made for each area of distinct lithology in the core section. The smear slides were examined by petrographic microscope. The archive half of the core section was then photographed.

After the cores were sampled and described, they were maintained in cold storage aboard *Glomar Challenger* until transferred to the DSDP repository. Core sections that were removed for organic-geochemistry study were frozen immediately aboard ship and kept frozen. All Leg 89 cores and frozen cores are stored at the DSDP West Coast Repository (Scripps Institution of Oceanography).

Rock and sediment obtained from core catchers and not used in the initial examination were retained in core liners for subsequent work. Sometimes significant pieces from the core were extracted and stored separately in labeled containers.

Visual core descriptions, smear-slide descriptions, and carbonate-bomb (% CaCO₃) determinations (all done aboard ship) provide the data for the core descriptions in this volume. This information is summarized and sample locations in the core are indicated on the core-description forms (Fig. 7).

Sediments and Sedimentary Rocks Core-Description Forms

Drilling Disturbance

Recovered strata, particularly soft sediments, may be extremely disturbed by drilling. This mechanical disturbance is a result of the coring technique, which uses a 25-cm-diameter bit with a 6-cm-diameter opening for the core sample. Symbols for the four disturbance categories used for soft and firm sediment are shown in Figure 7 in the column of the core-description form headed "Drilling Disturbance." These symbols are used on the core-description sheets. The disturbance categories are defined as (1) slightly deformed: bedding contacts are slightly bent; (2) moderately deformed: bedding contacts have undergone extreme bowing, and firm sediment is fractured; (3) very deformed: bedding is completely disturbed or homogenized by drilling, sometimes showing symmetrical diapirlike structure; and (4) soupy: water-saturated intervals have lost all aspects of original bedding; (5) breccia: indurated sediments are broken into angular fragments by the drilling process, perhaps along preexisting fractures; and (6) biscuited: sediments are

firm and are broken into discs about 5 to 10 cm in length.

Sedimentary Structures

In the soft, and even in some harder, sedimentary cores, it may be extremely difficult to distinguish between natural structures and structures created by the coring process. Thus the description of sedimentary structures was optional. Locations and types of structures appear as graphic symbols in the column headed "Sedimentary Structures" on the core-description form (Fig. 7). Figures 8 and 9 give the keys to these symbols.

Color

Colors of the core samples are determined using the Geological Society of America Rock-Color Chart (Munsell system). Colors were determined immediately after the cores were split and while wet.

Lithology

The graphic column on the core-description form is based on the lithologies and represented by a single pattern or by a grouping of two or more symbols. The symbols in a grouping correspond to end-members of sediment constituents, such as clay or nannofossil ooze. The symbols are shown in the graphic column in approximate proportions to the lithologies in the core. Figure 9 shows the symbols used to denote lithologies in the graphic lithology columns of core-description forms.

Concentrations of smear-slide (or thin-section) components, carbonate content (% CaCO₃), and organic carbon content determined on board are listed below the core description; the two numbers separated by a hyphen refer to the section and centimeter interval, respectively, of the sample. The locations of these samples in the core and a key to the codes used to identify these samples are given in the column headed "Samples" (Fig. 7). Locations and intervals of organic geochemistry (OG), interstitial water (IW), and physical property (PP) samples are presented in the "Graphic Lithology" column.

Lithologic Classification

Introduction

The sediment classification used on Leg 89 differs somewhat from that recommended by the JOIDES Panel on Sedimentary Petrology and Physical Properties (SPPP), mainly in the naming of intermediate mixtures of nonbiogenic, siliceous biogenic, and/or calcareous biogenic components. As a first approximation, we considered each sediment to be a mixture of these three components. The SPPP classification (described in its entirety in the Leg 42, Part 2 *Initial Reports*, Ross, Ne-prochnov, et al., 1978) provides specific guidelines for classifying nonbiogenic components, and we have not modified this classification, which is essentially that of Shepard (1954; Fig. 10). In our classification, the term "clay" is used for any material less than 4 μm in size

SITE		HOLE				CORE		CORED INTERVAL				
TIME - ROCK UNIT	BIOSTRATIGRAPHIC ZONE	FOSSIL CHARACTER				SECTION	METERS	GRAPHIC LITHOLOGY	DRILLING DISTURBANCE	SEDIMENTARY STRUCTURES	SAMPLES	LITHOLOGIC DESCRIPTION
		FORAMINIFERS	NANNOFOSSILS	RADIOLIARIANS	DIATOMS							
	(N) = Nannofossil Zones	(F) = Foraminifer Zones	(R) = Radiolarian Zones	(D) = Diatom Zones		0.5 1.0						<p>Lithologic Description</p> <p>Organic carbon and carbonate content Section-depth (cm), % organic carbon, % CaCO₃</p> <p>Smear slide summary Section-depth (cm) (M) = Minor lithology (D) = Dominant lithology (T) = Thin section CF = Coarse fraction Texture: % Sand, silt, clay Components: %</p> <p>↑ Interstitial water sample ↓</p> <p>↑ Organic geochemistry sample ↓</p>
						2	IW					
						3		See key to graphic lithology symbols (Figure 9)				
						4	OG					
						5						
						6						
						7						
					CC							

Figure 7. Sample core form description of sediment (barrel sheet).

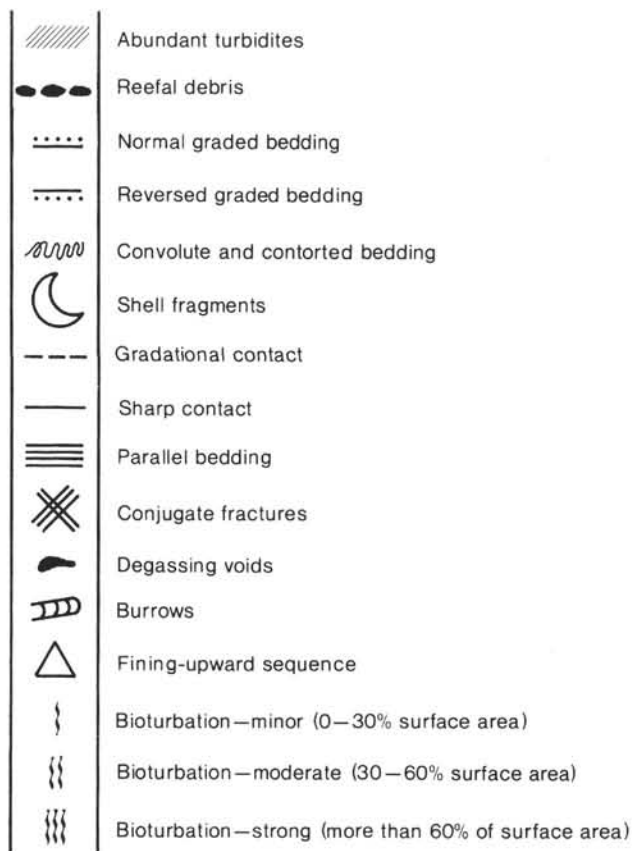


Figure 8. Symbols of sedimentary structures used on core-description forms (sediment).

without regard to composition or origin (hence, terms such as “pelagic clay” do not appear in our classification).

Our modifications of the SPPP classification are aimed at: (1) making the naming of mixtures of nonbiogenic, siliceous biogenic, and calcareous biogenic components internally consistent, and (2) providing names for intermediate mixtures of these three components. Our classification of the three-component system of nonbiogenic, siliceous biogenic, and calcareous biogenic is shown in Figure 11, using the example of clay as the dominant nonbiogenic component, nannofossils as the dominant calcareous biogenic component, and diatoms as the dominant siliceous biogenic component.

Rules for Using Classification

1. 10–25% of a component qualifies it for “minor-modifier” (“-bearing”) status.

2. 25–50% of a component qualifies it for “major-modifier” status. Major modifiers are: (a) Nonbiogenic: silty, clayey, sandy, muddy, and so on. (b) Calcareous biogenic: nannofossil, foraminifer, or simply calcareous (but it is best to be more specific where possible). (c) Siliceous biogenic: diatom (or diatomaceous), radiolarian, or siliceous (again, it is best to be as specific as possible).

3. 50% of a component or group of components (e.g., total siliceous biogenic or total calcareous biogenic) de-

termines the “main name.” Main names are: (a) Nonbiogenic: if the total of nonbiogenic components is greater than 50%, the main name is determined by the dominant size(s) (Fig. 11). Examples of nonbiogenic main names are clay, silt, silty clay, sand, mud, and so forth. (b) Biogenic: if the total of biogenic components is greater than 50%, the main name is ooze.

4. The most abundant component appears closest to the main name. Major and minor modifiers are listed in order of increasing abundance to the left of the main name. Some examples are: (a) 60% nannofossils, 30% foraminifers, 5% radiolarians, 5% clay = foraminifer-nannofossil ooze; (b) 40% nannofossil, 35% foraminifers, 15% radiolarians, 10% clay = clay- and radiolarian-bearing foraminifer-nannofossil ooze; (c) 30% foraminifers, 15% radiolarians, 30% sand, 25% silt = radiolarian-bearing foraminifer silty sand; (d) 40% diatoms, 30% nannofossils, 30% clay = clayey nannofossil diatom ooze or nannofossil clayey diatom ooze.

Other Sediment Types

This lithologic classification covers the majority of unconsolidated sediment types likely to be found in deep-sea areas. A few less common sediment types encountered during Leg 89 are worth mentioning here.

Volcanogenic Sediments

Volcanogenic sediments may consist of primary volcanic components (e.g., volcanic glass, feldspar, pyroxene, volcanic rock fragments, opaque minerals, etc.) or secondary minerals (e.g., smectites, palagonite, zeolites, palygorskite, celadonite, etc.) (Vallier and Kidd, 1977). Volcanogenic sediments are not usually found as distinct beds except when deposited by air-fall right after a large eruption, or, more commonly, when deposited by downslope transport (e.g., turbidity currents and debris flows) on volcanic edifices (e.g., Line Islands, Schlanger, Jackson, et al., 1976; Mid-Pacific Mountains, Vallier and Jefferson, 1981) and in adjacent basins (e.g., Nauru Basin, Moberly and Jenkyns, 1981; Mariana Basin, this volume). Most wind-borne volcanogenic sediments are masked by biogenic components and terrigenous components and are recognized mainly by the textures of the glass or altered glass; the presence of certain minerals in smear slides or, more commonly, on X-ray diffractograms helps identify them. Hyaloclastites are fragmental rocks that form when fluid lava is quickly quenched and shattered as it contacts seawater, resulting in broken pieces of basaltic glass (Williams and McBirney, 1979).

Zeolites

This sedimentary component commonly appears in smear slides as clear to cloudy euhedral fibrous to lathlike crystals with negative optical relief. Zeolites are authigenic hydrous aluminosilicates and are usually found in slowly accumulating deep-sea pelagic clay or at depth in volcanogenic deposits. The most common zeolites in deep-sea sediments are phillipsite and clinoptilolite, with phillipsite usually being the more abundant in young sediments and clinoptilolite more abundant in deeper, older layers. Zeolites are usually associated with ferromanga-

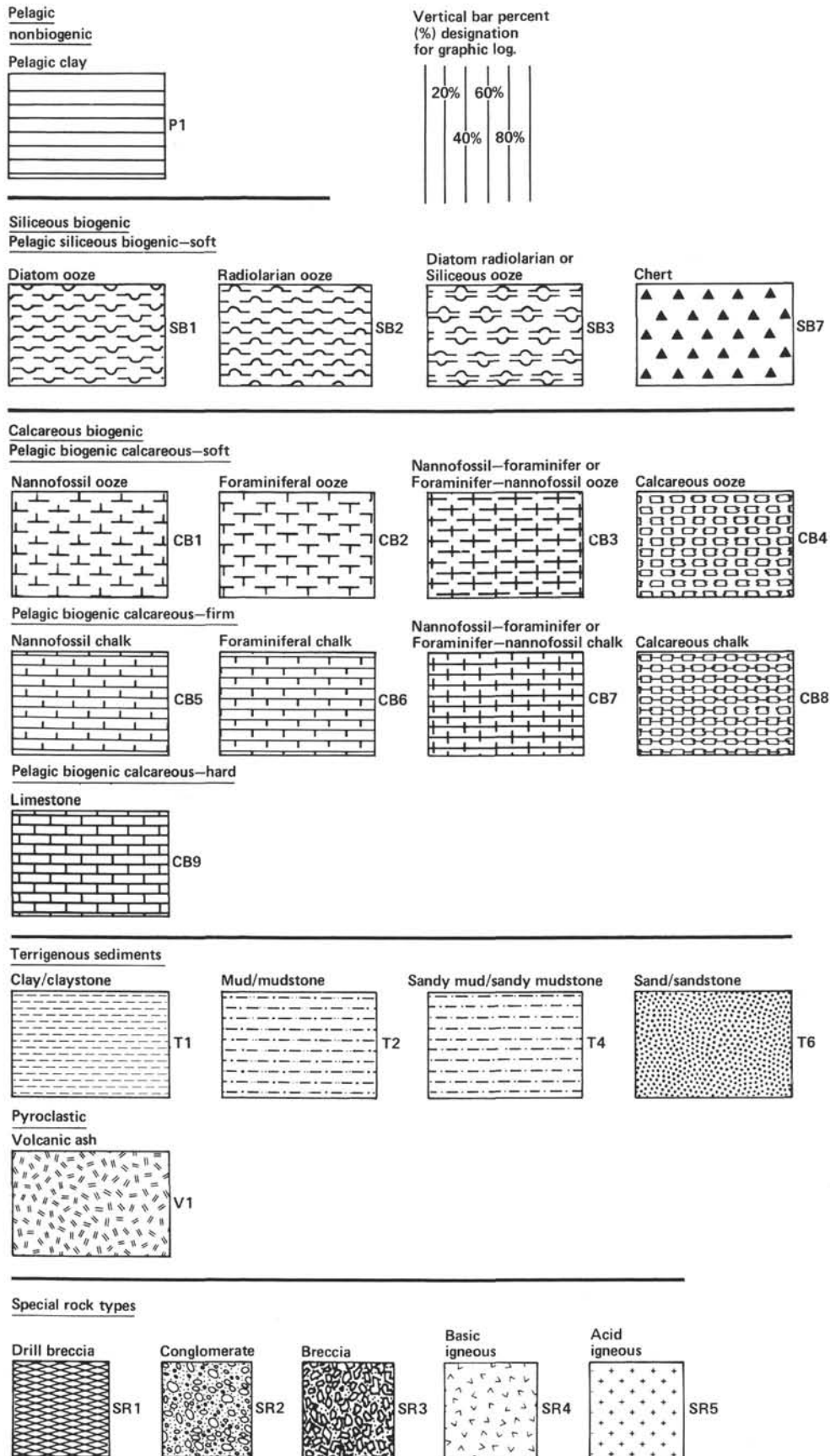


Figure 9. Symbols used in graphic lithology columns of core-description form (sediment).

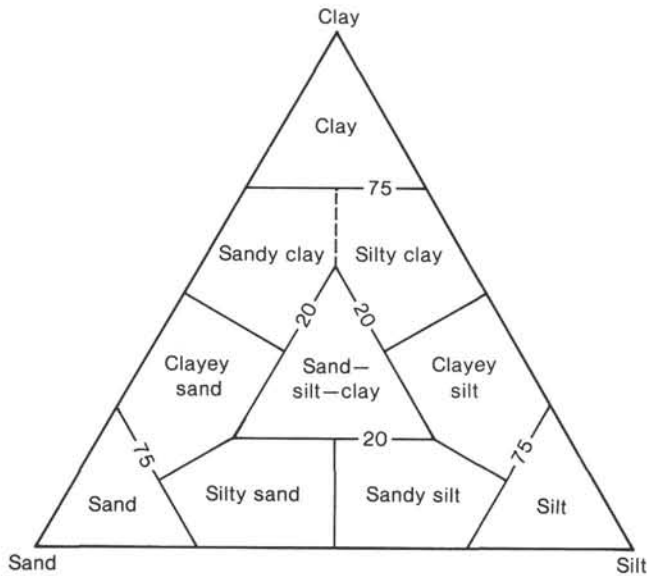


Figure 10. Textural classification of clastic sediments.

nese oxides, smectite clays, palagonite, and other primary or secondary volcanogenic minerals, and most zeolites probably form from alteration of volcanogenic materials.

Degree of Induration

Recognizing stages in the degree of induration of a sediment can provide valuable insight into the processes

of diagenesis and lithification. For carbonate sediments, a three-fold induration scale (soft, firm, hard—equivalent to ooze, chalk, and limestone) has been in use for many years. No such scale exists for noncarbonate sediments; they are either sediment or rock. The general criteria for recognizing the three stages on induration in carbonate sediments are as follows:

soft (ooze): sediment has little strength and is easily deformed with the blade of a spatula

firm (chalk): partly indurated ooze; can be easily scratched or deformed with the edge of a spatula blade

hard (limestone): completely cemented rock

For nonbiogenic sediments (mostly silt and clay), it is usually sufficient to stick with the two-fold induration scale of (1) sediment, and (2) rock, which is identified by the suffix “-stone” following the main sediment name.

For siliceous sediments, there may be a need for a classification of sediment of intermediate induration equivalent to chalk used for carbonate sediments. “Diatomite” is commonly used as a good working field term for a partly indurated, weakly cemented rock composed mainly of diatom frustules. “Radiolarian sand” is a term we applied to firm sediment containing abundant radiolarians. Hard, lithified siliceous sediments are “porcellanite” and “chert”. Porcellanite is usually dull, brown to white, fairly porous, and may contain clay, zeolites, or carbonate. Chert, in contrast, is lustrous, has conchoidal fractures, and is much denser and harder than porcellanite. These two siliceous rock types usually can

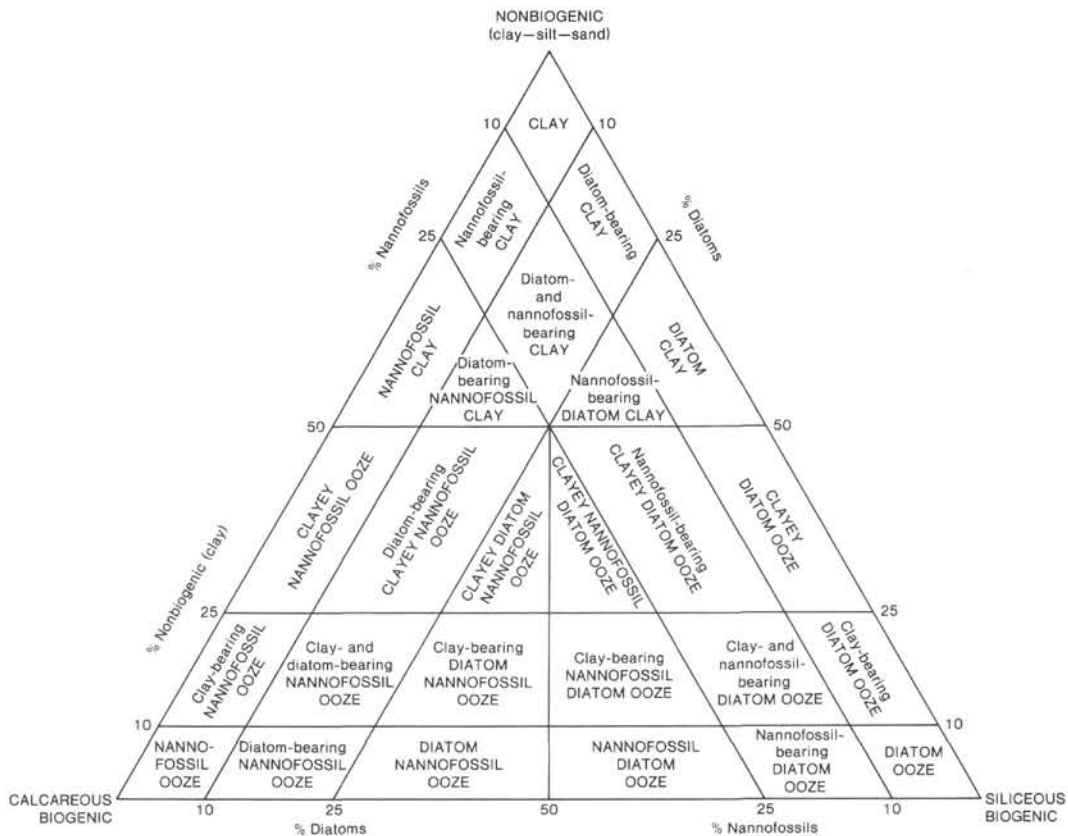


Figure 11. Sediment classification for use of Leg 89.

be readily distinguished in hand specimen and are sufficient for shipboard descriptions. More detailed descriptions require detailed studies involving thin sections, scanning electron microscopy, X-ray diffraction, and chemical analyses. In some of our descriptions of lithologies recovered on Leg 89, we have also used the genetic term silicified limestone to designate siliceous limestone or porcellanite that was once a carbonate ooze but has been partly cemented by silica into a very hard rock.

Igneous Rock Nomenclature

The terminology used in the igneous rock section is based mainly on mineralogy and texture and comprises standard terms. Graphic symbols used for designating igneous rocks, degree of alteration, and miscellaneous other features are shown in Figure 12.

Basaltic rocks are termed aphyric (0% phenocrysts), sparsely phytic (1–2% phenocrysts), and moderately phytic (>10% phenocrysts) on the basis of an examination with hand lens or binocular microscope (~10×). Glomerophytic is used to denote clusters of phenocrysts. If a few phenocrysts are found scattered throughout a section generally lacking phenocrysts, the material is described as aphyric. This system allows the division of basalt sequences into units with distinctive or persistent visual differences. Basalts are further subdivided by phenocryst type, for example, olivine moderately phytic basalt.

As diabase was frequently encountered in the “flow-sill complex,” it is given a separate symbol, as are special features that are present in a sill such as cumulate zones of granophyre patches.

The breccia symbol mainly denotes breccia composed of basaltic fragments or recognizable broken pillows with glassy rims. Partly dislocated pillow fragments may be set in an altered hyaloclastite or carbonate matrix.

The core descriptions also indicate the location of samples taken for various analyses (Fig. 7).

X-Ray Diffraction

Shipboard X-ray diffraction analysis was carried out on a Rigaku machine with a Cu tube that produces Cu-K α radiation at 30 kV, 10 mA. The best and most consistent results were obtained by using smear-mounted slides containing a small amount of sylvite (KCl) or quartz (SiO₂) as an internal standard. Smear mounts were prepared by making a suspension of the material in acetone or water and applying the suspension to a glass slide, which was then air dried. A correction factor to calculate 2 θ degree angles was determined by comparing accepted peak values for the internal standard to those peaks observed in the smear mounts. Diffractograms were usually obtained by scanning from about 55° to 7° 2 θ .

Biostratigraphy and Basis for Age Determination

Microfossil zonation of sediments cored on Leg 89 is based on the scheme outlined in Figures 13 and 14.

The following letters are used on core-description sheets to indicate fossil abundance:

A = abundant (many species and specimens)

C = common (many species, easy to make age assignment)

R = rare (enough for age assignment)

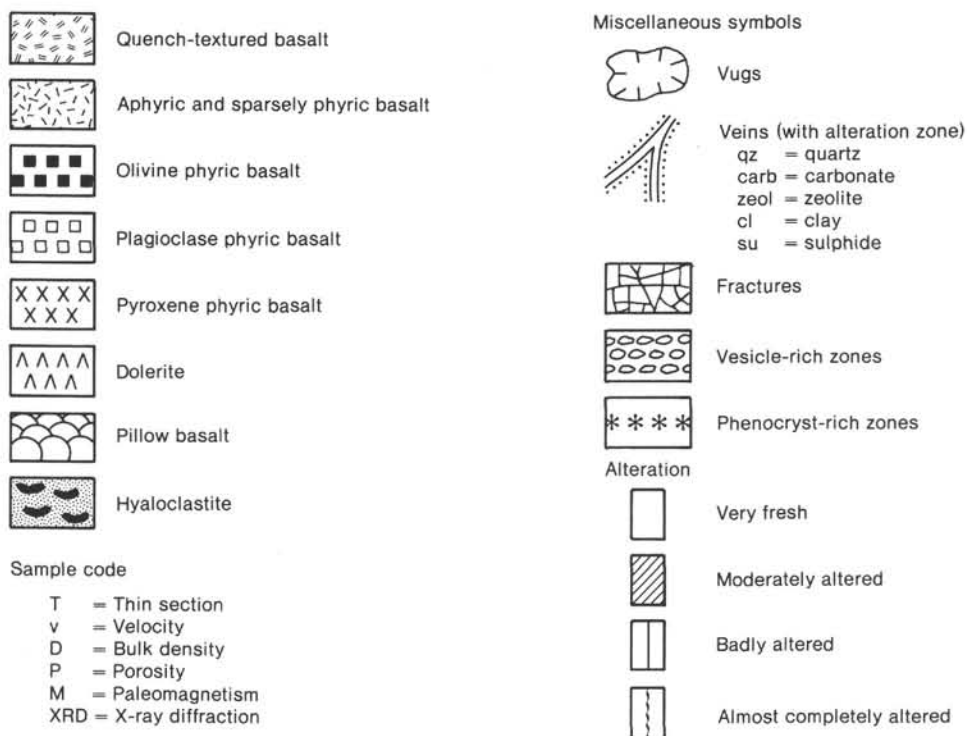


Figure 12. Graphic symbols used to designate rock type, degree of alteration, and other features of igneous rocks recovered on Leg 89.

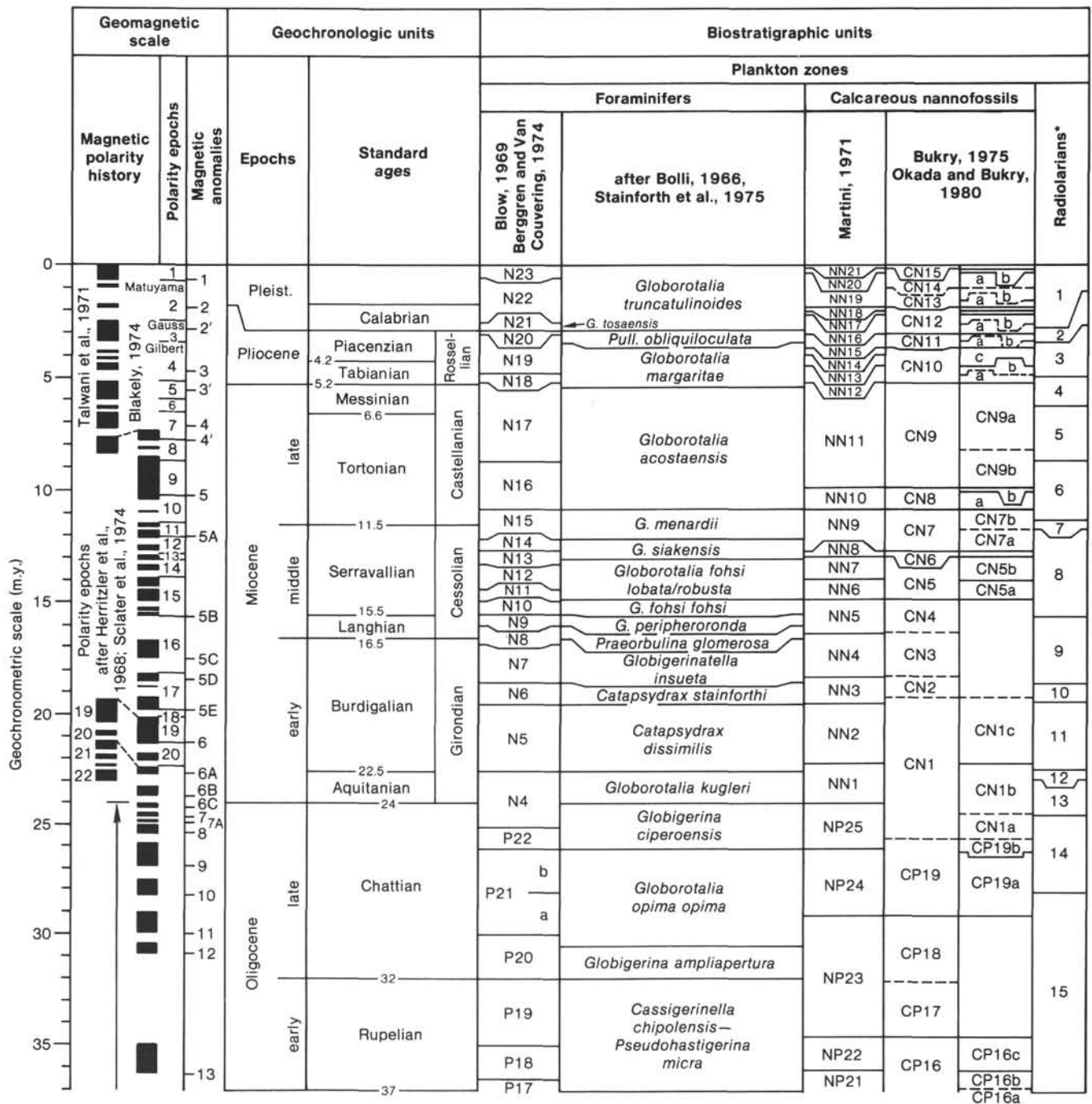


Figure 13. Tertiary biostratigraphic scheme compiled after Hardenbol and Berggren, 1978: absolute age and chronology; Blow, 1969, Berggren and Van Couvering, 1974, Bolli, 1966, Stainforth et al., 1975, modified after Lowrie et al., 1982: planktonic foraminifers; Martini, 1971, Bukry, 1975, Okada and Bukry, 1980: calcareous nannoplankton; Riedel and Sanfilippo, 1978, Westberg and Riedel, 1978, Nigrini, 1977, Theyer et al., 1978: radiolarians; Alvarez et al., 1977, Lowrie et al., 1982: Paleogene magnetic sequence; Heirtzler et al., 1968, Sclater et al., 1974, Blakely, 1974, Talwani et al., 1971: Neogene to Recent magnetic sequence.

T = trace (few species and specimens, not enough for age assignment)
 B = barren

P = poor (substantial or very strong evidence of dissolution, abrasion, recrystallization)

Letters used to designate fossil preservation are:

- E = excellent (no dissolution or abrasion)
- G = good (very little dissolution or abrasion)
- M = moderate (dissolution, abrasion, recrystallization very noticeable)

Shipboard Geochemical Measurements

Interstitial waters were routinely analyzed for pH, alkalinity, salinity, calcium, magnesium, and chlorinity. The sediment was squeezed with a stainless steel press. The water was collected in a plastic syringe, and then filtered through a 0.45- μ m millipore filter.

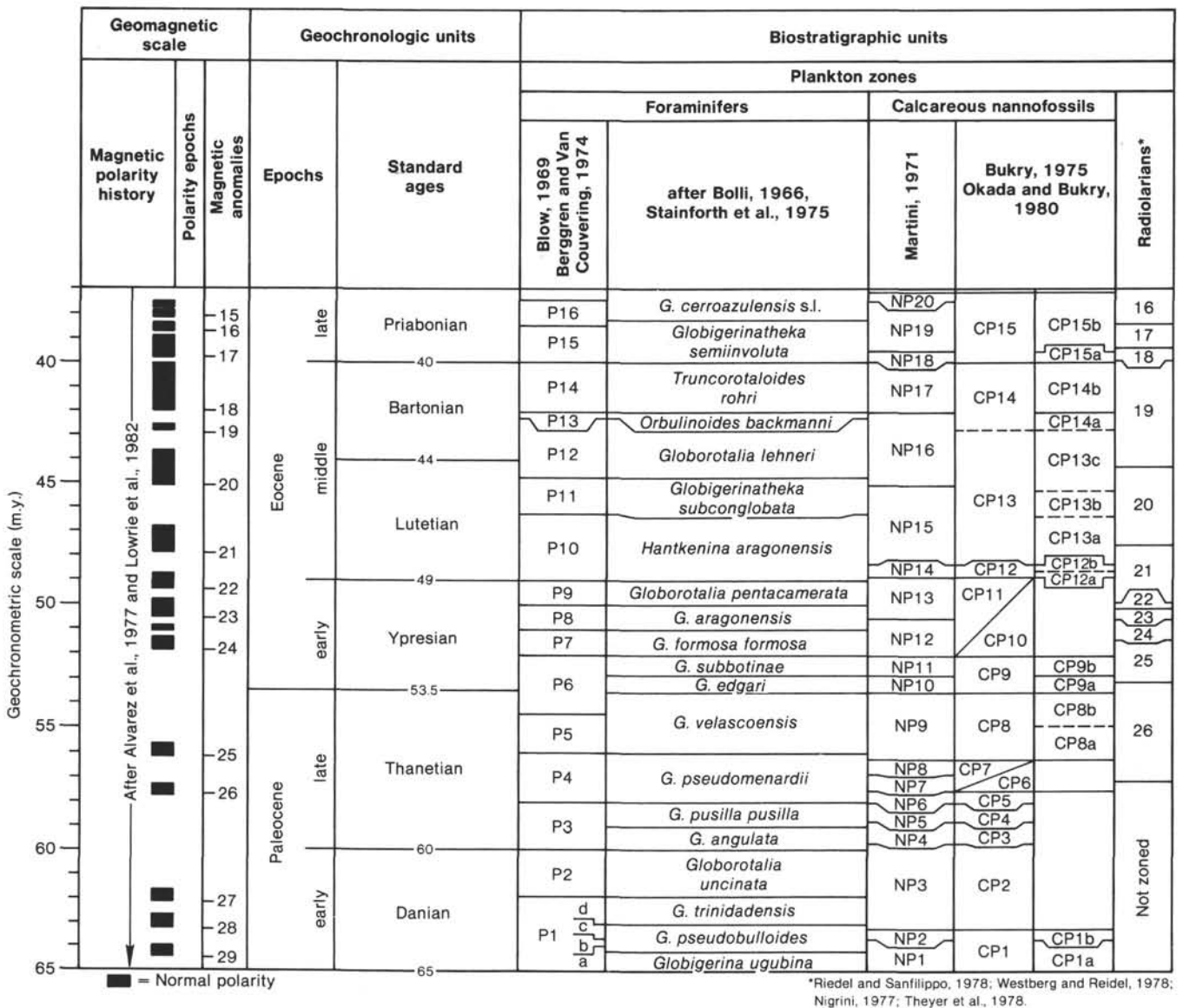


Figure 13 (continued).

Values of pH were determined using a Corning Model 130 pH meter and a Markson combination electrode calibrated with 4.01 and 7.42 buffer standards. All readings originally were in millivolts and later were converted to pH values. All pH measurements were made in conjunction with alkalinity measurements.

Alkalinity concentrations were determined potentiometrically. Five- to ten-ml samples were first tested for pH, then titrated with 0.1 N HCl. Near the end-point, acid was added in 0.01-ml or 0.005-ml increments and the millivolt readings noted for each increment. The exact end-point was then calculated using the Gran Factor method (Gieskes and Rogers, 1973).

Salinity was calculated from the fluid refractive index, as measured by a Goldberg optical refractometer, using the expression:

$$\text{Salinity (\%)} = 0.55 \times \Delta N$$

where ΔN is the refractive index multiplied by 10^4 . The refractometer's calibration is checked periodically using IAPSO seawater standard and deionized water.

Calcium ion concentration was measured by titrating a 0.5-ml sample with EGTA using GHA as an indicator. To sharpen the end-point, the calcium-GHA complex was extracted into a layer of butanol. No correction was made for strontium, which is also included in the result.

Magnesium ion concentration was measured by titrating a buffered 0.5-ml sample to an Eriochrome Black-T end-point, using EDTA (sodium salt) as a titrant. This method analyzes all alkaline earths, including calcium, magnesium, strontium, and barium; concentrations are obtained by subtracting the calcium (which includes strontium) from this analysis.

Chlorinity is determined by titrating a 0.1-ml sample, diluted with 1 ml deionized water, with silver nitrate to a potassium chromate end-point.

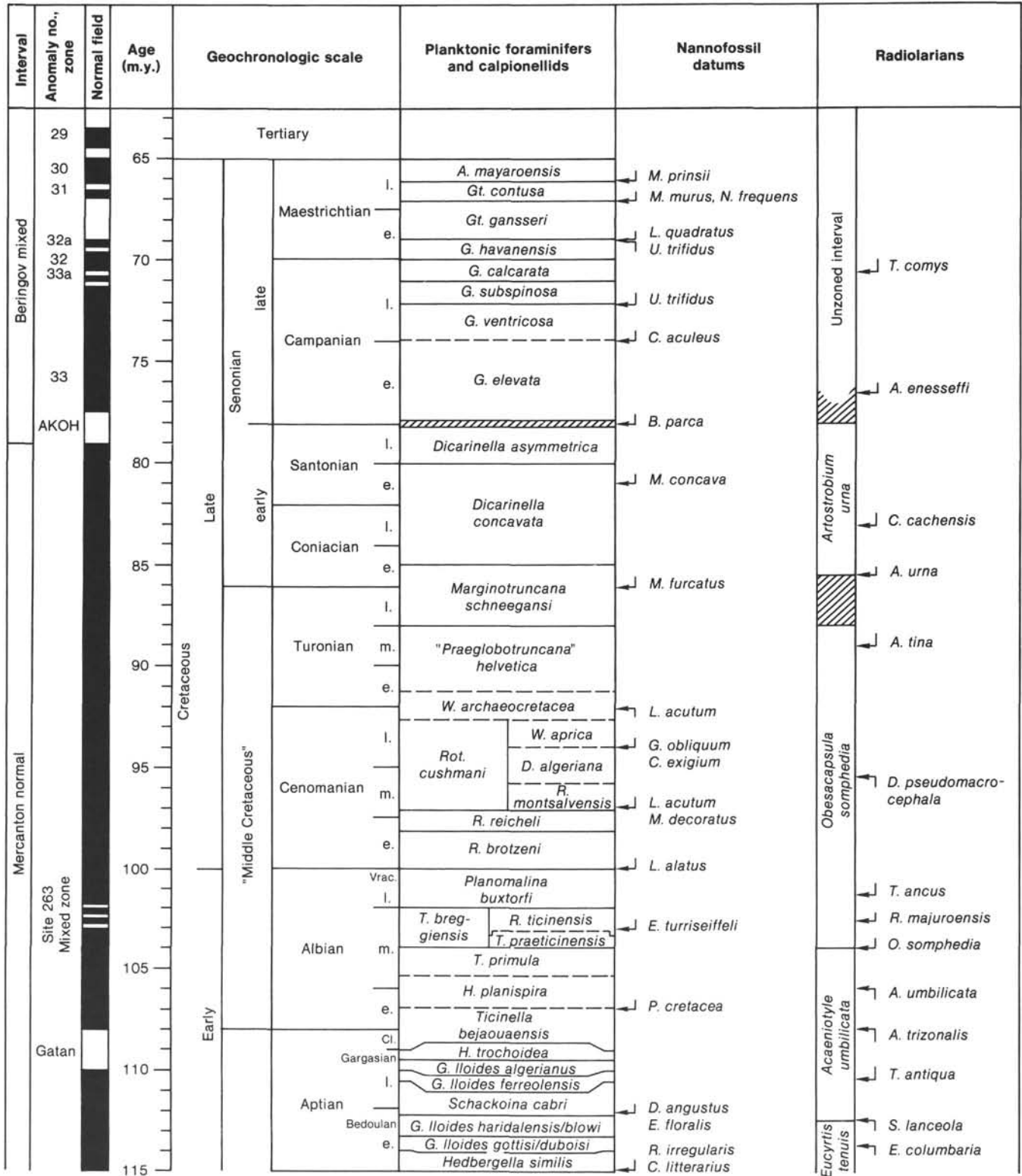


Figure 14. Mesozoic biostratigraphic scheme compiled after van Hinte, 1976: absolute age, chronology and Cretaceous magnetic sequence; Premoli Silva and Sliter, 1981 (modified): planktonic foraminifers; Remane, 1978: calpionellids; Thierstein, 1976 (TH), Perch-Nielsen, 1979, Medd, 1982 (M), Barnard and Hay, 1974 (B + H): calcareous nannoplankton; Riedel and Sanfilippo, 1974, Schaaf, 1981: radiolarians; Bryan et al., 1980, Cande et al., 1978: Jurassic magnetic sequence.

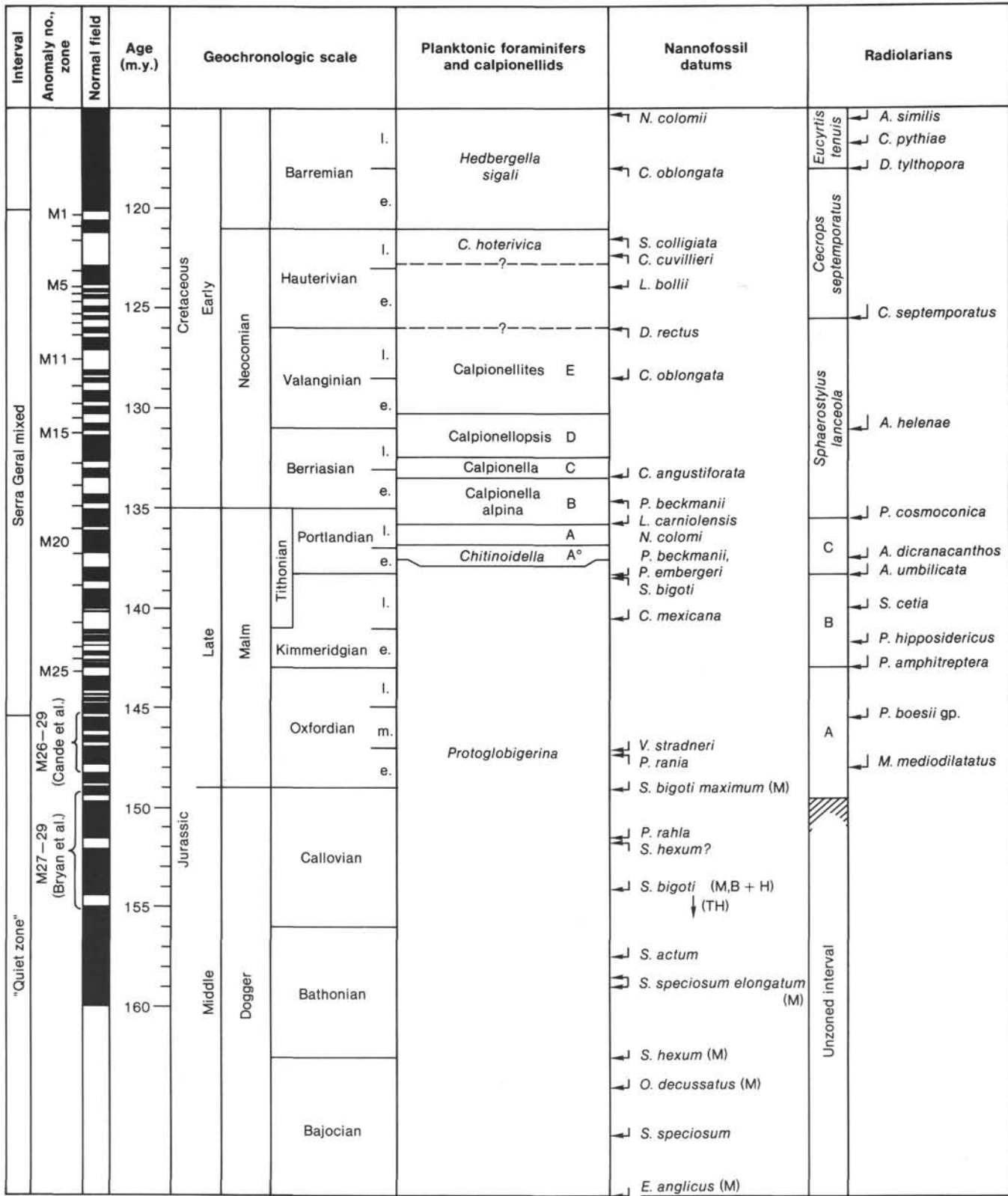


Figure 14 (continued).

Methods and equipment were checked and standardized at each site using IAPSO standard seawater. As a further check, a surface seawater sample was analyzed and archived. This sample also was used to test for possible drill-water contamination of the interstitial water samples.

Carbonate Bomb

Percent CaCO_3 was also determined on board ship by the "Karbonate Bombe" technique (Müller and Gastner, 1971). In this simple procedure, a sample is powdered and treated with HCl in a closed cylinder. Any resulting CO_2 pressure is proportional to the CaCO_3 content of the sample. Application of the calibration factor to the manometer reading ($\times 100$) yields percent CaCO_3 . Percent error can be as low as 1% for sediments high in CaCO_3 , and in general an accuracy of about 2 to 5% can be obtained.

These data are presented on the core-description sheets. The sample interval is designated by two numbers: the section number, followed by the top of the centimeter interval. For example, a sample from Section 2, 11 to 12 cm, with 90% calcium carbonate will be represented on the core-description sheet as "2, 11-12 (90%)."

Physical Properties—Procedures

A thorough discussion of physical properties is presented by Boyce (1976) with respect to equipment, methods, errors, correction factors, and problems related to coring disturbance. Only a brief review of methods employed on Leg 89 is given here.

Velocity

Compressional wave velocity was measured on the Hamilton Frame velocimeter by timing a 400-kHz pulse between two transducers and by measuring the distance across the sample with a dial gauge. Measurements were made at laboratory temperature and pressure. With consolidated sediments, a piece was removed from the core and trimmed carefully to form two parallel surfaces to ensure good contact with the transducer heads. Water was used to make good acoustical contact between the sample and the transducers.

Calibration of the velocimeter consisted of making numerous measurements through lucite, aluminum, and brass standards of varying thicknesses to obtain a calibration constant for each of 3- $\mu\text{s}/\text{cm}$ settings on the DSDP Tektronix 485 oscilloscope used to make the traveltime measurements. This calibration constant reflects the position picked by the operator as representing the first break from horizontal of the sonic signal. Data from the calibrations remained constant throughout the duration of our stay at each Leg 89 site.

For hard sediments and rocks, minicores were cut and the surfaces were carefully ground flat to make measurements possible for both horizontal and vertical directions.

GRAPE Density

The Gamma Ray Attenuation and Porosity Evaluator (GRAPE) was used to determine wet bulk density

based on the attenuation of gamma rays by the sample. Boyce (1976) discusses the theoretical aspects in detail. During Leg 89 GRAPE was used in two modes: (1) continuous GRAPE, in which most sections of the core were irradiated; continuous "corrected" wet bulk density (relative to quartz) was plotted on an analog graph; and (2) two-minute GRAPE, in which the gamma count through a small piece of the core was measured for 2 min., followed by a similar count through air and/or a quartz standard.

Continuous GRAPE

Prior to running each core through the device, an aluminum standard was measured. A density of 2.60 Mg/m^3 was assigned to the 6.61-cm (diameter) aluminum standard analog record, and a density of 1.0 Mg/m^3 to the 2.54-cm (diameter) aluminum standard analog record. Linear interpolation of the GRAPE analog data between these values yielded an "empirical" wet bulk density of the sediment sample in the core (ρ_{bcz}). If the sample completely filled the core, then $\rho_{bc} =$ "corrected" wet bulk density (relative to quartz). Then:

$$\rho_b = \frac{(\rho_{bc} - \rho_{fc}) - \rho_\gamma - (\rho_f)}{(\rho_{gc} - \rho_{fc})} + \rho_f$$

where $\rho_g =$ true grain density ($\approx 2.65 \text{ Mg}/\text{m}^3$ for sediments), although actual grain densities were determined subsequently to range from 2.18 to 2.80 Mg/m^3 ; $\rho_{gc} =$ corrected grain density ($\approx 2.7 \text{ Mg}/\text{m}^3$ for sediments); $\rho_f =$ true fluid density ($\approx 1.025 \text{ Mg}/\text{m}^3$); $\rho_{fc} =$ corrected fluid density ($\approx 1.125 \text{ Mg}/\text{m}^3$); and $\rho_b =$ true wet bulk density.

Using these values,

$$\rho_b = 1.066 (\rho_{bc} - 1.125) + 1.025 \quad (1)$$

Shipboard reduction of analog GRAPE records involved (1) selection of high-density portions of each core section on the analog record, and (2) calculation of true wet bulk density (ρ_b) by formula (1). These calculations were subsequently corrected for independently determined true grain density. Porosity (ϕ) is obtained by

$$\phi(\%) = \frac{\rho_g - \rho_b}{\rho_g - \rho_f} \times 100.$$

Two-Minute GRAPE

For two-minute GRAPE calculations,

$$\rho_{bc} = \frac{\ln(I_0/I)}{d \mu qtz}$$

where $I_0 =$ two-minute gamma count through air, $I =$ two-minute gamma count through the sample, $d =$ gamma ray path length through the sample, and $\mu qtz =$ quartz attenuation coefficient determined daily by measuring through a quartz standard. Then, as in the continuous GRAPE calculation (assuming a 2.65 grain density),

$$\rho_b = 1.066 (\rho_{bc} - 1.125) + 1.025$$

and

$$\phi(\%) = \frac{100(2.65 - \rho_b)}{1.675}$$

Boyce (1976) estimates $\pm 5\%$ accuracy for continuous GRAPE data and $\pm 2\%$ for two-minute GRAPE data.

Samples for the two-minute GRAPE counts were also used for gravimetric methods. In harder sediments, when increased induration allowed, minicores were cut from the drilling biscuits and coherent sections, and the surfaces were carefully trimmed.

Gravimetric Technique: Boyce Cylinder, Chunk and Minicore

Following the two-minute GRAPE counts, the samples prepared as just described were used for water content and porosity determinations. No salt corrections were applied in any of these techniques. Drying and weighing equipment on board *Glomar Challenger* was used for these measurements.

$$\text{Water content (percent wet weight)} = 100 \times \frac{[(\text{weight wet sediment}) - (\text{weight dry sediment})]}{(\text{weight wet sediment})}$$

For porosity determinations, a grain density of 2.65 Mg/m³ and a water density of 1.03 Mg/m³ were assumed.

$$\text{Porosity (\%)} = 100 \times \frac{\text{volume of evaporated water}}{\text{volume of wet sediment}} = 100 \times \frac{[(\text{weight of evaporated water}) / (1.03 \text{ Mg/m}^3)]}{\left[\frac{(\text{weight of dry sediment})}{(2.65 \text{ Mg/m}^3)} + \frac{(\text{weight evaporated water})}{(1.03 \text{ Mg/m}^3)} \right]}$$

The porosity calculations were subsequently corrected for independently determined true grain densities.

Magnetic Susceptibility

After alternative-field demagnetization for basalt minicores, magnetic susceptibility was measured aboard ship by a Bison susceptibility bridge (Model 3101). By using a minicore holder, measurements were made in three mutually perpendicular directions by averaging measured values of six directions. More detailed analyses were made on shore and described in Fujii and Hamano (this volume).

Paleomagnetism

Natural remanent magnetization (NRM) of minicore samples was measured aboard ship on a Digico Fluxgate magnetometer by J. Ogg. More precise analyses using progressive demagnetization were performed on cryogenic magnetometers in magnetic-field-free laboratories onshore. Methods and results are discussed in the site reports and Ogg (this volume).

Photography

Sets of color and black and white negatives of whole cores are available for consultation. In addition, nega-

tives in black and white for closeup documentation of special structures are archived at DSDP.

Obtaining Samples

Potential investigators who desire to obtain samples should refer to the DSDP-NSF Sample Distribution Policy. Sample request forms may be obtained from the Curator, Deep Sea Drilling Project, A-031, University of California at San Diego, La Jolla, California 92093. Requests must be as specific as possible: include site, core section, interval within a section, and volume of sample required.

REFERENCES

- Alvarez, W., Arthur, M. A., Fischer, A. G., Lowrie, W., Napoleone, G., Premoli Silva, I., and Roggenthen, W. M., 1977. Upper Cretaceous-Paleocene magnetic stratigraphy at Gubbio, Italy. V. Type section for the Late Cretaceous-Paleocene geomagnetic reversal time scale. *Geol. Soc. Am. Bull.*, 88:383-389.
- Barnard, T., and Hay, W. W., 1974. On Jurassic coccoliths: a tentative zonation of the Jurassic of Southern England and North France. *Eclogae Geol. Helv.*, 67:563-585.
- Berggren, W. A., and Van Couvering, J. A., 1974. *The Late Neogene*: Amsterdam (Elsevier Scientific Publishing Co.).
- Blakely, R. J., 1974. Geomagnetic reversals and crustal spreading rates during the Miocene. *J. Geophys. Res.*, 79:2979-2985.
- Blow, W. H., 1969. Late middle Eocene to Recent planktonic foraminiferal biostratigraphy. In Bronnimann, P., and Renz, H. H. (Eds.), *Proc. First Int. Conf. Planktonic Microfossils*: Leiden (E. J. Brill), pp. 199-241.
- Bolli, H. M., 1966. Zonation of Cretaceous to Pliocene marine sediments based on planktonic foraminifera. *Assoc. Venezolana de Geologica, Minería y Petroleo*, 9:1-32.
- Boyce, R. E., 1976. Definitions and laboratory techniques of compressional sound velocity parameters and wet-water content, wet-bulk density, and porosity parameters by gravimetric and gamma ray attenuation techniques. In Schlanger, S. O., Jackson, E. D., et al., *Init. Repts. DSDP*, 33: Washington (U.S. Govt. Printing Office), 931-958.
- Bryan, G. M., Markl, R. G., and Sheridan, R. E., 1980. IPOD site surveys in the Blake-Bahama Basin. *Mar. Geol.*, 35:43-63.
- Bukry, D., 1975. Coccolith and silicoflagellate stratigraphy, northwestern Pacific Ocean, Deep Sea Drilling Project Leg 32. In Larson, R. L., Moberly, R., et al., *Init. Repts. DSDP*, 32: Washington (U.S. Govt. Printing Office), 677-701.
- Cande, S. C., Larson, R. L., and LaBrecque, S. L., 1978. Magnetic lineations in the Pacific Jurassic quiet zones. *Earth Planet. Sci. Lett.*, 41:434-441.
- Gieskes, J. M., and Rogers, W. C., 1973. Alkalinity determination in interstitial waters of marine sediments. *J. Sed. Petrol.*, 43: 272-277.
- Hardenbol, J., and Berggren, W. A., 1978. A new Paleogene numerical time scale. In Cohee, G. V. et al. (Eds.), *Contributions to the Geological Time Scale*. Am. Assoc. Pet. Geol. Bull., Studies in Geology, (6)213-234.
- Heirtzler, J. R., Dickson, G. O., Herron, E. M., Pitman, W. C., III, and Le Pichon, X., 1968. Marine magnetic anomalies, geomagnetic field reversals, and motion of the ocean floor and continents. *J. Geophys. Res.*, 73:2119-2136.
- Lowrie, W., Alvarez, W., Napoleone, G., Perch-Nielsen, K., Premoli Silva, I., and Toumarkine, M., 1982. Paleogene magnetic stratigraphy in Umbrian carbonate rocks. The Contesa section, Gubbio. *Geol. Soc. Am. Bull.*, 93:414-432.
- Martini, E., 1971. Standard Tertiary and Quaternary calcareous nanoplankton zonation. *Second Plankt. Conf., Roma*, pp. 739-785.
- Matthews, D. J., 1939. *Tables of the velocity of sound in pure water and in seawater*: Admiralty, London (Hydrographic Department).
- Medd, A. W., 1982. Nannofossil zonation of the English Middle and Upper Jurassic. *Mar. Micropaleontol.*, 7:73-95.
- Moberly, R., and Jenkyns, H. C., 1981. Cretaceous volcanogenic sediments of the Nauru Basin, Deep Sea Drilling Project Leg 61. In

- Larson, R. L., Schlanger, S. O., et al., *Init. Repts. DSDP*, 61: Washington (U.S. Govt. Printing Office), 533-548.
- Müller, G., and Gastner, M., 1971. The "Karbonate-Bombe," a simple device for determination of the carbonate content in sediments, soils, and other materials. *J. Jahrb. Mineral. Monatsh.*, 10:466-469.
- Nigrini, C., 1977. Tropical Cenozoic Artostrobiidae (Radiolaria). *Micropaleontology*, 23(3):241-269.
- Ogg, J. G., and Steiner, M. B., 1984. Jurassic magnetic polarity pattern: time scale and reversal frequency. *Int. Geol. Cong., Moscow, Session C20*.
- Okada, H., and Bukry, D., 1980. Supplementary modification and introduction of code numbers to the low-latitude coccolith biostratigraphic zonation (Bukry, 1973, 1975). *Mar. Micropaleontol.*, 5: 321-325.
- Premoli Silva, I., and Sliter, W. V., 1981. Cretaceous planktonic foraminifers from the Nauru Basin, Leg 61, Site 462, western equatorial Pacific. In Larson, R. L., Schlanger, S. O., et al., *Init. Repts. DSDP*, 61: Washington (U.S. Govt. Printing Office), 423-437.
- Remane, J., 1978. Calpionellids. In Haq, B. U., and Boersma, A., *Introduction to Marine Micropaleontology*: New York (Elsevier), pp. 161-170.
- Riedel, W. R., and Sanfilippo, A., 1974. Radiolaria from the southern Indian Ocean, Leg 26. In Davies, T. A., Luyendyk, B. P., et al., *Init. Repts. DSDP*, 26: Washington (U.S. Govt. Printing Office), 771-813.
- Riedel, W. R., and Sanfilippo, A., 1978. Stratigraphy and evolution of tropical Cenozoic radiolarians. *Micropaleontology*, 24(1):61-96.
- Ross, D. A., Neprochnov, Y. P., et al., 1978. *Init. Repts. DSDP*, 42, Pt. 2: Washington (U.S. Govt. Printing Office).
- Schaaf, A., 1981. Late Early Cretaceous Radiolaria from Deep Sea Drilling Project Leg 62. In Thiede, J., Vallier, T. L., et al., *Init. Repts. DSDP*, 62: Washington (U.S. Govt. Printing Office), 419-470.
- Sclater, J. G., Gerald, R. D., McGowran, B., and Gartner, S., 1974. Comparison of the magnetic and biostratigraphic time scales since the Late Cretaceous. In von der Borch, C. C., Sclater, J. G., et al., *Init. Repts. DSDP*, 22: Washington (U.S. Govt. Printing Office), 381-386.
- Schlanger, S. O., Jackson, E. D., et al., 1976 *Init. Repts. DSDP*, 33: Washington (U.S. Govt. Printing Office).
- Shepard, F. P., 1954. Nomenclature based on sand-silt-clay ratios. *J. Sed. Petrol.*, 24:151-158.
- Shiple, T. H., Whitman, J. M., Duennebie, F. K., Petersen, L. D., 1983. Seismic stratigraphy and sedimentation history of the East Mariana Basin, western Pacific. *Earth Planet Sci. Lett.*, 64: 257-275.
- Stainforth, R. M., Lamb, J. L., Luterbacher, H. P., Beard, J. H., and Jeffords, R. M., 1975. Cenozoic planktonic foraminiferal zonation and characteristics of index forms. *Univ. Kansas Paleontol. Contrib.*, Article 62, Vols. 1 and 2.
- Steiner, M. B., 1981. Paleomagnetism of the igneous complex, Site 462. In Larson, R. L., Schlanger, S. O., et al., *Init. Repts. DSDP*, 61: Washington (U.S. Govt. Printing Office), 717-730.
- Talwani, M., Winisch, C. C., and Langseth, M. G., 1971. Reykjanes Ridge crest: a detailed geophysical study. *J. Geophys. Res.*, 76: 473-517.
- Theyer, F., Mato, C. Y., and Hammond, S. K., 1978. Paleomagnetic and geochronologic calibration of latest Oligocene to Pliocene radiolarian events, equatorial Pacific. *Mar. Micropaleontol.*, 3: 377-395.
- Vallier, T. L., and Jefferson, W. D., 1981. Volcanogenic sediments from Hess Rise and the Mid-Pacific Mountains, Deep Sea Drilling Project, Leg 62. In Thiede, J., Vallier, T. L., et al., *Init. Repts. DSDP*, 62: Washington (U.S. Govt. Printing Office), 545-558.
- Vallier, T. L., and Kidd, R. B., 1977. Volcanogenic sediments in the Indian Ocean. In Heirtzler, J. R. (Ed.), *Indian Ocean Geology and Biostratigraphy*: Washington (Am. Geophys. Union), pp. 87-118.
- van Hinte, J. E., 1976. A Cretaceous time scale. *Bull. Am. Assoc. Pet. Geol.*, 60:498-516.
- Westberg, M. J., and Riedel, W. R., 1978. Accuracy of radiolarian correlations in the Pacific Miocene. *Micropaleontology*, 24:1-23.
- Williams, H., and McBirney, A. R., 1979. *Volcanology*: San Francisco (Freeman, Cooper, and Co.).